SEEEP2022 Program Summer School

Helium cryogenics for superconducting cooling

Shiran Bao

Zhejiang University, Hangzhou, China

National High Magnetic Field Laboratory, Tallahassee, FL, USA

08/17/2022

Cryoboat Group

Institute of Refrigeration and Cryogenics

College of Energy Engineering, Zhejiang University

Research topics:

Liquid hydrogen
Air separation
Cryocooler
Helium cryogenics

Group Leader: Prof. Limin Qiu

Researchers: Prof. Kai Wang Prof. Xiaoqin Zhi Prof. Shiran Bao

Postdoc: Dr. Shaolong Zhu Dr. Hanying Jiang Dr. Song Fang

Over 20 graduate students

A group attracted to cold

Cryoboat

Content

①

He II and Quantum hydrodynamics

① Specificity of helium and superfluid helium (He II)

- Lowest melting and boiling points of all the elements.
- Helium does not solidify at atmospheric pressure.

Peter Kapitza, Nobel Prize in Physics 1978

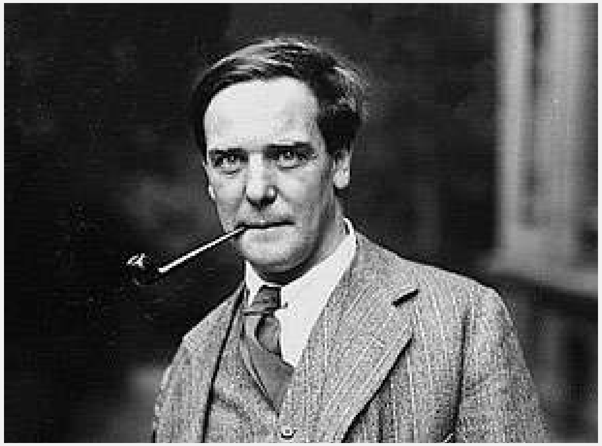

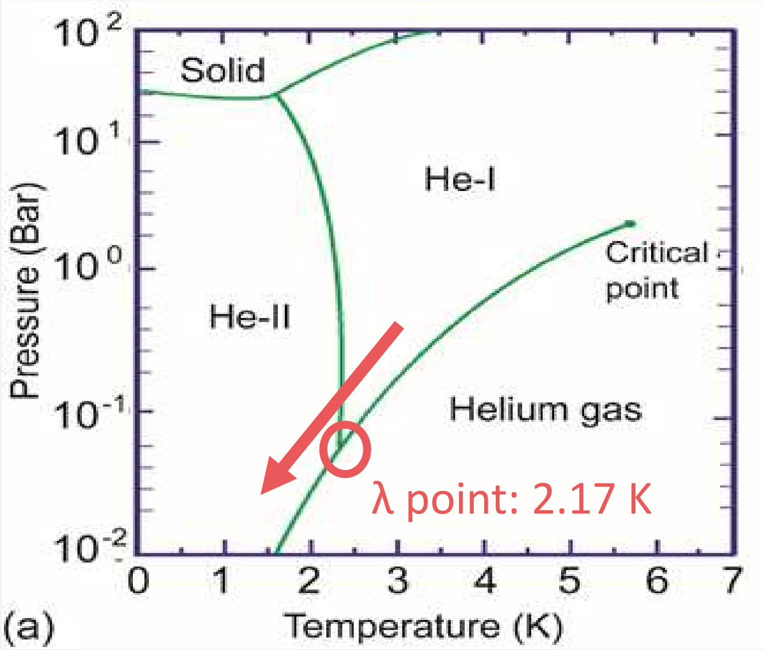

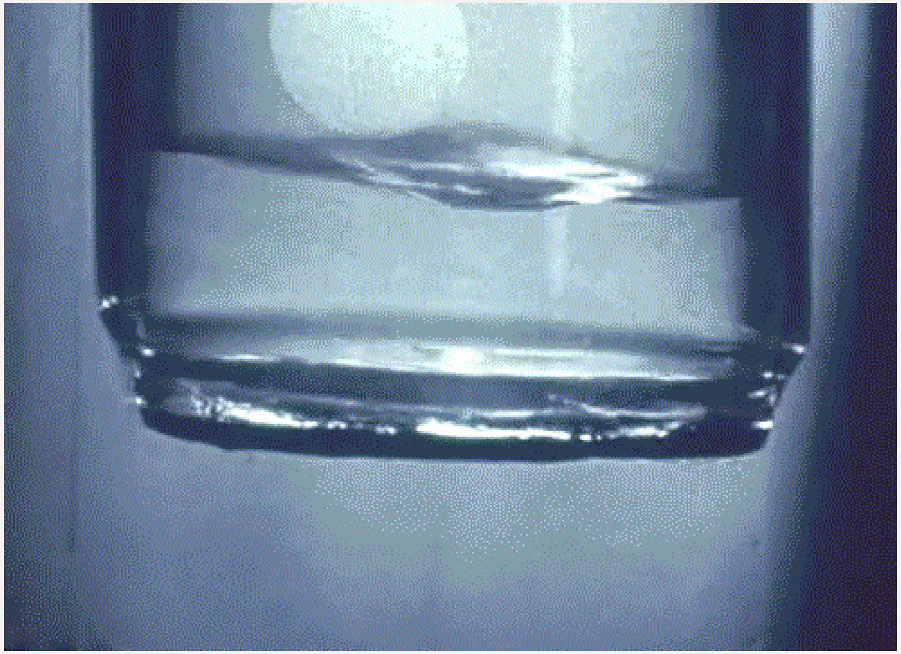

Superfluid helium (He II) as a coolant

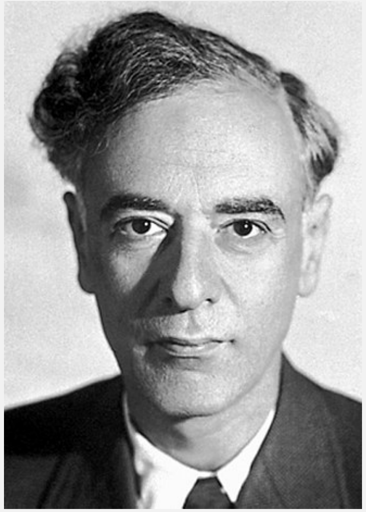

Lev Landau, Nobel Prize in Physics 1962

There exist two components in He II:

- Superfluid component (condensate)
- Normal-fluid component (excitations)

	Density	Velocity	Viscosity	Entropy
Superfluid	$\rho_s(T)$	$\mathbf{v}_s(\mathbf{r})$	0	0
Normal fluid	$\rho_n(T)$	$\mathbf{v}_n(\mathbf{r})$	$\eta_n(T)$	$s_n(T)$

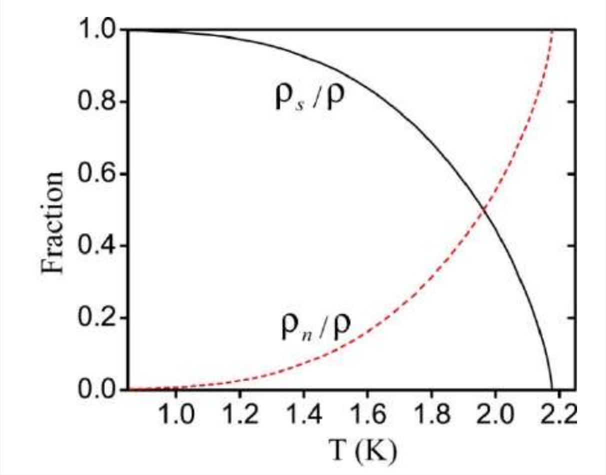

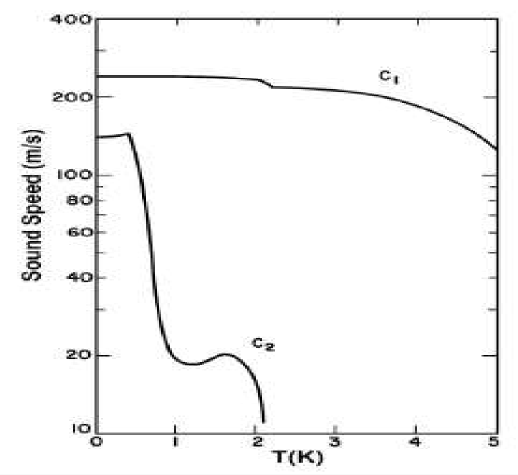

Two sound modes:

- 1st sound: two fluids move in phase
- 2nd sound: two fluids move out of phase

Quantum and classical turbulence in He II

- Superfluid turbulence is a random tangle of quantized vortices.

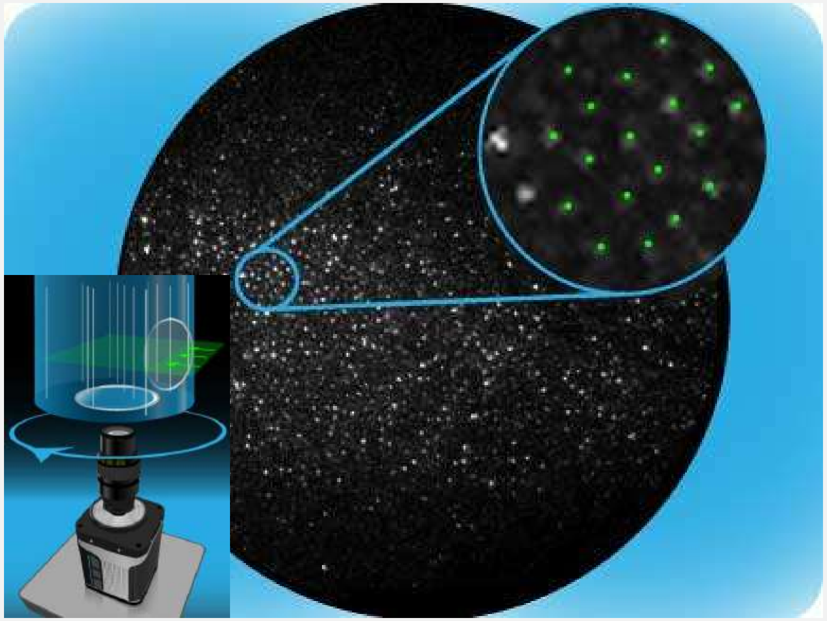

Quantum turbulence

Each vortex has the same conserved circulation. QT is thus simpler to model than classical turbulence.

- Turbulence in normal fluid can be affected by the quantized vortices.

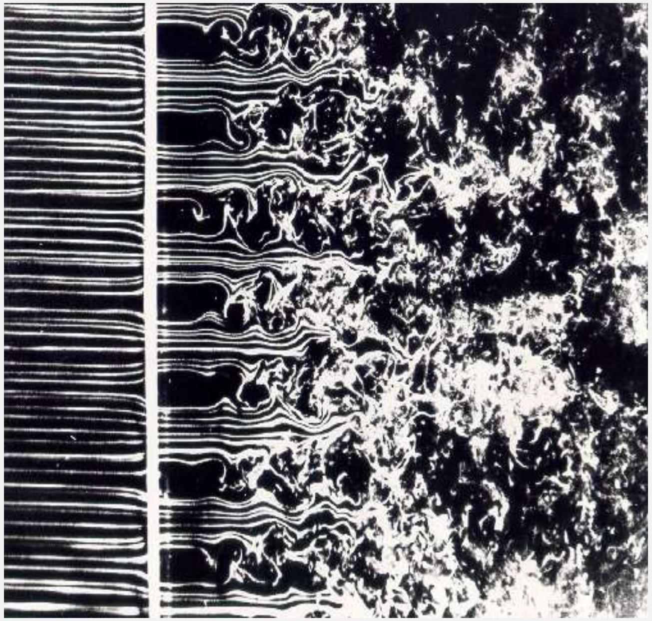

Classical turbulence

Quasi-particles can interact with vortices → origin of many peculiar hydrodynamics in the two-fluid system.

Quantum hydrodynamics: (1) Above 1 K (two-fluid regime)

- Heat transfer in He-II is by counterflow :

  the superfluid moves towards the source of heat;

  the normal fluid flows in the opposite direction, carrying thermal energy.

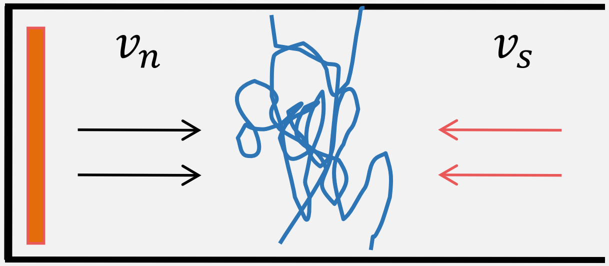

$$v_n = \frac{w/A}{\rho S T} \qquad v_s = \frac{\rho_n}{\rho_s} v_n$$

Turbulence in counterflow can affect the heat transfer !

He-II has been used as a coolant:

Maglab:

Superconducting Magnets – 45T hybrid; 900Hz NMR; 32 T; etc.

CERN: LHC

(27 Km ring)

LHe-4: 700,000 liters

T=1.8 K

Quantum hydrodynamics: (2) Below 0.6 K: (Pure QT)

- At low T when there is no normal fluid, the decay of QT energy at scales smaller than vortex spacing is believed to be via Kelvin wave cascade.

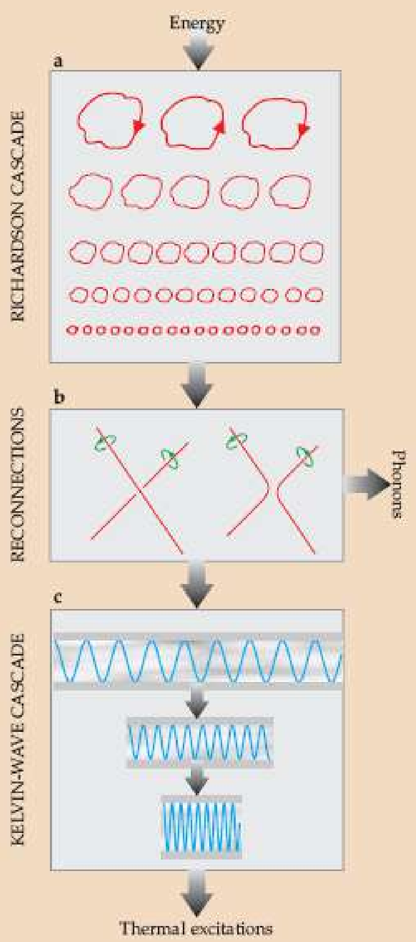

Figure 4. How quantum turbulence might evolve in a superfluid at very low temperature.[15] (a) First, turbulent energy mechanically injected at large length scale flows to ever smaller length scales in a quasiclassical Richardson cascade, down to length scale ℓ, the typical distance between quantized vortex lines. (b) Then vortex-line reconnection comes into play. The reconnection is modestly dissipative, producing some phonon emission. But more of the energy goes into generating Kelvin waves of vortices (c). Strong nonlinear interactions make the Kelvin waves cascade down to wavelengths short enough so that their energy can be dissipated as phonons or other thermal excitations. Aspects of this picture are still controversial.

(1) Classical turbulent energy spectrum is indicated but no direct determination.

$$dE/dt = -\nu\omega^2 = -\nu_{eff}(\kappa L)^2$$

(2) What is the spectrum in the Kelvin wave cascade regime ?

(3) Is there any bottleneck at the transition from classical cascade to Kelvin wave cascade ?

Direct vortex-line visualization at low T is urgently needed!

Do we really have a complete understanding of counterflow?

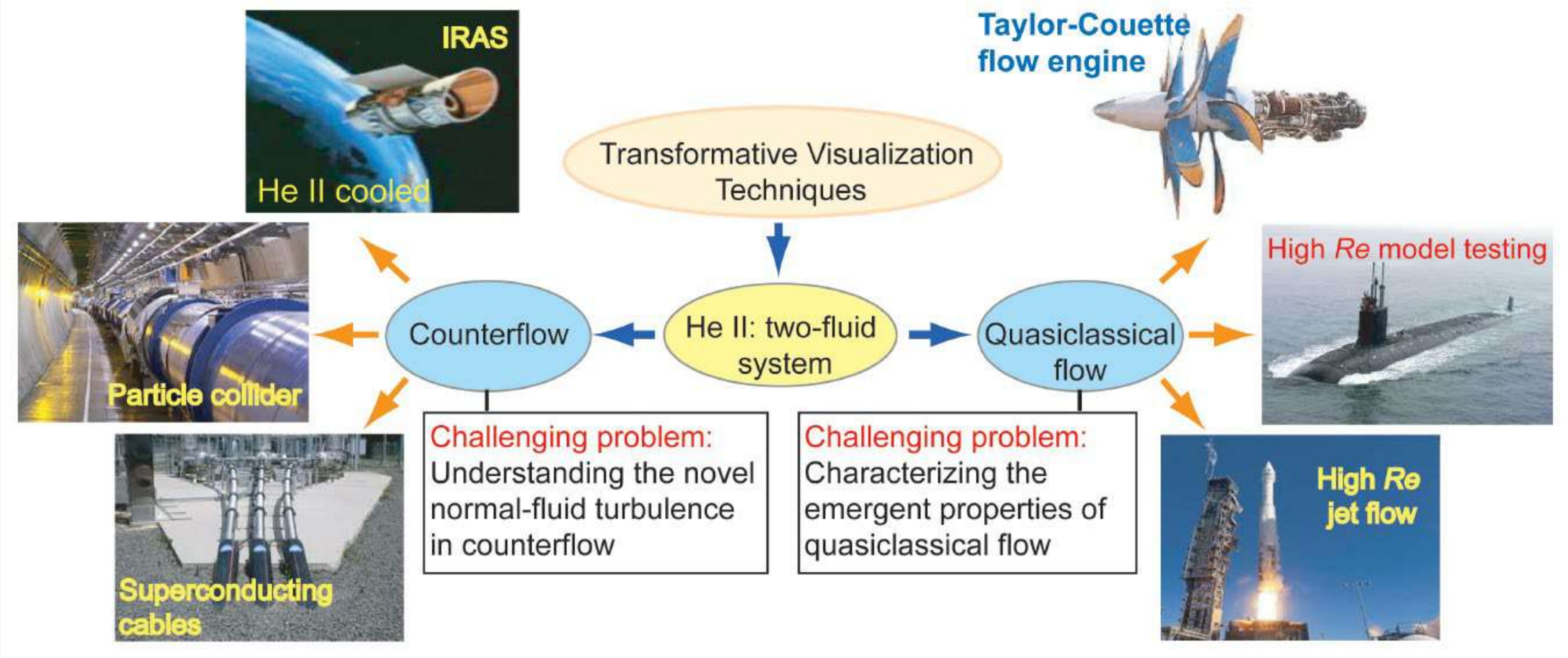

- Challenge: many tools developed for classical fluids are not applicable

We need tools that allow independent quantitative flow measurements in the two-fluid system!

②

Flow visualization studies in He II

- Particle imaging velocimetry (PIV) with polymer microspheres, solidified hydrogen ice particles

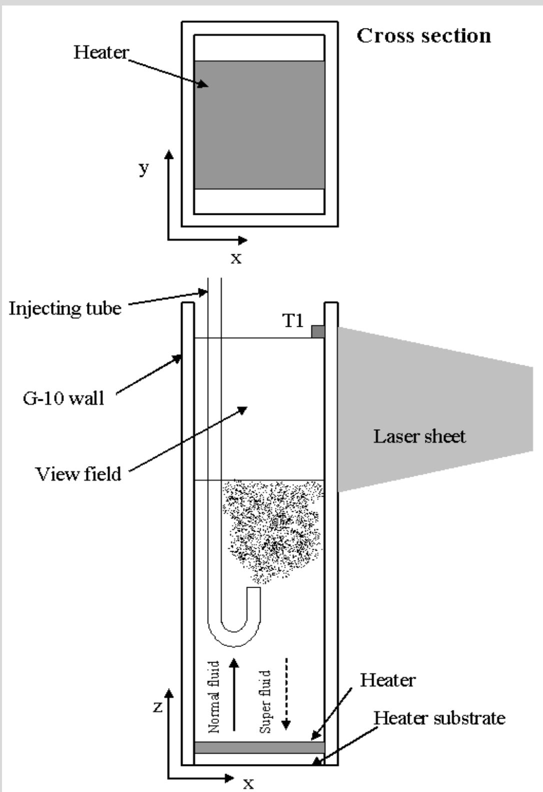

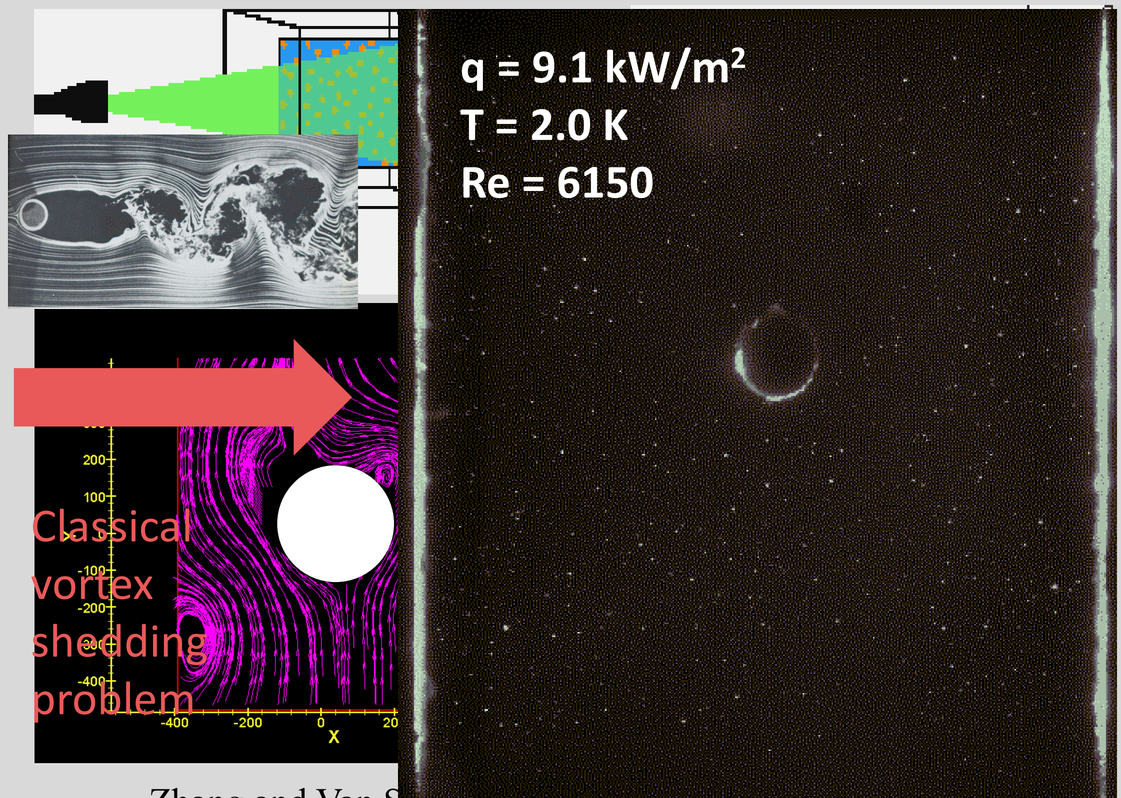

Zhang and Van S

②

PIV/PTV techniques using micron-sized tracers

- Particle tracking velocimetry (PTV, with hydrogen isotopes ice particles)

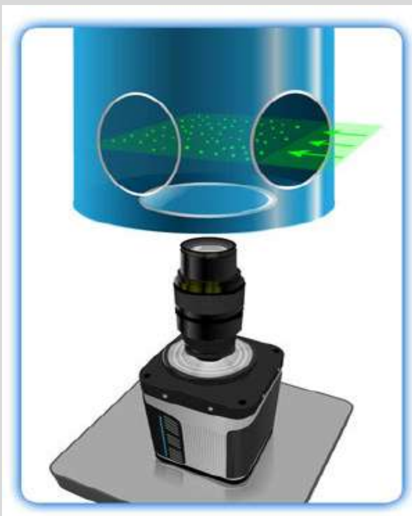

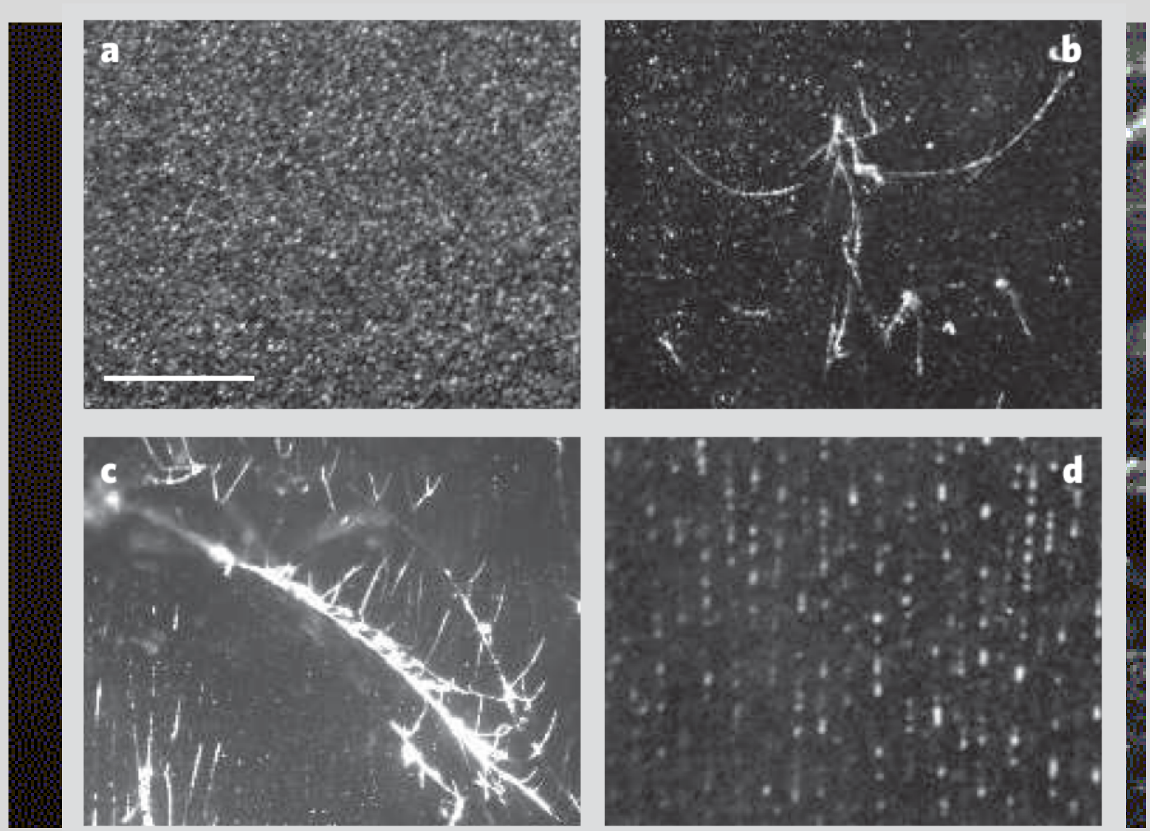

Direct visualization of quantized vortices: Particles are observed to bind on vortex lines due to Bernoulli’s effect

Bewley, Lathrop, and Sreenivasan *Nature* ***441,*** *588 (2006)*

PIV/PTV techniques using micron-sized tracers

- Our recent progress with PTV in He II:

1) Thermal counterflow:

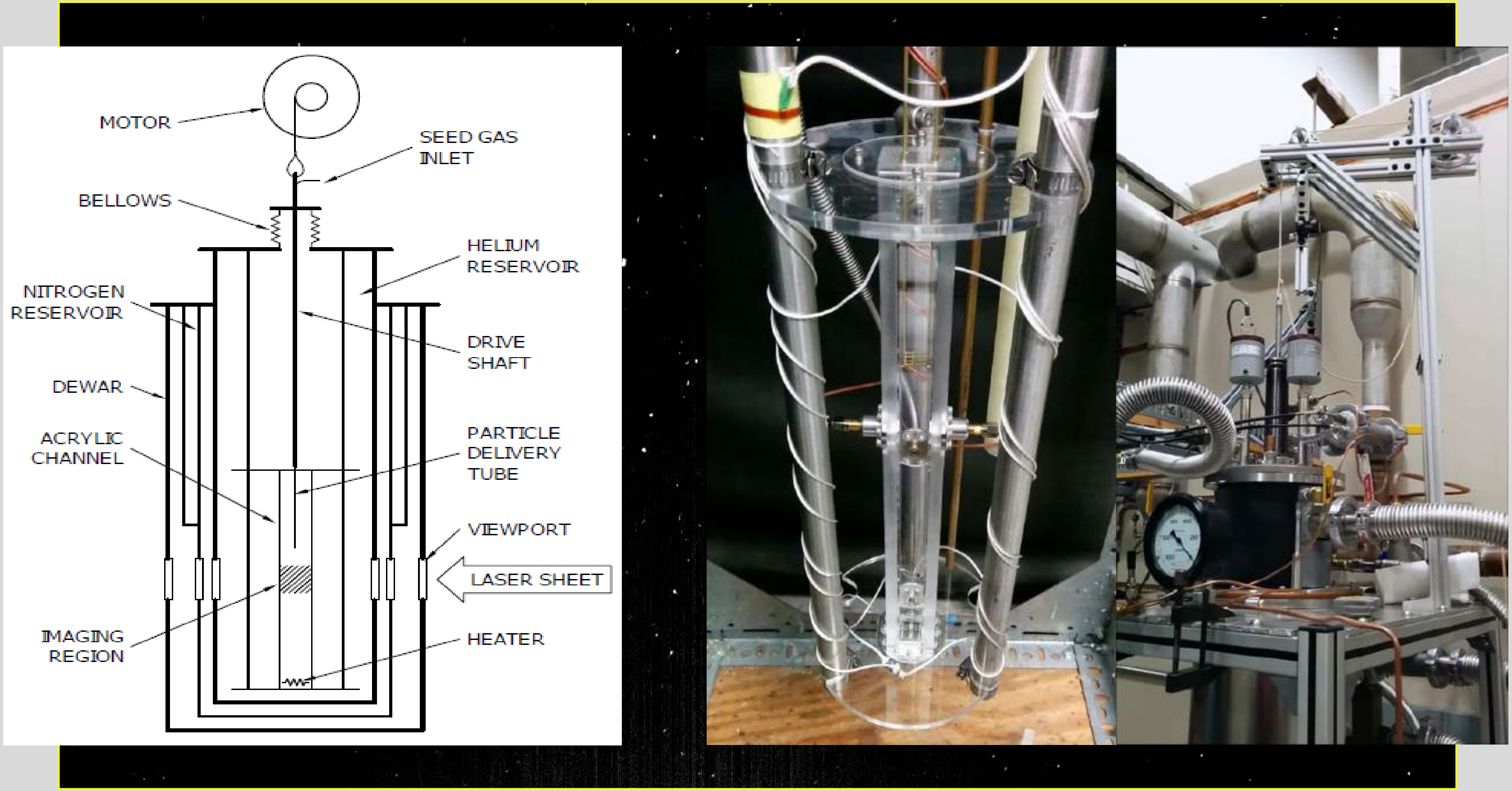

PIV/PTV techniques using micron-sized tracers

- Particle tracks and V_y pdfs show two distinct regimes
- Two peaks at low heat fluxes: G1 (lower velocity peak) and G2 (high velocity peak)
- One peak at high heat fluxes: G3

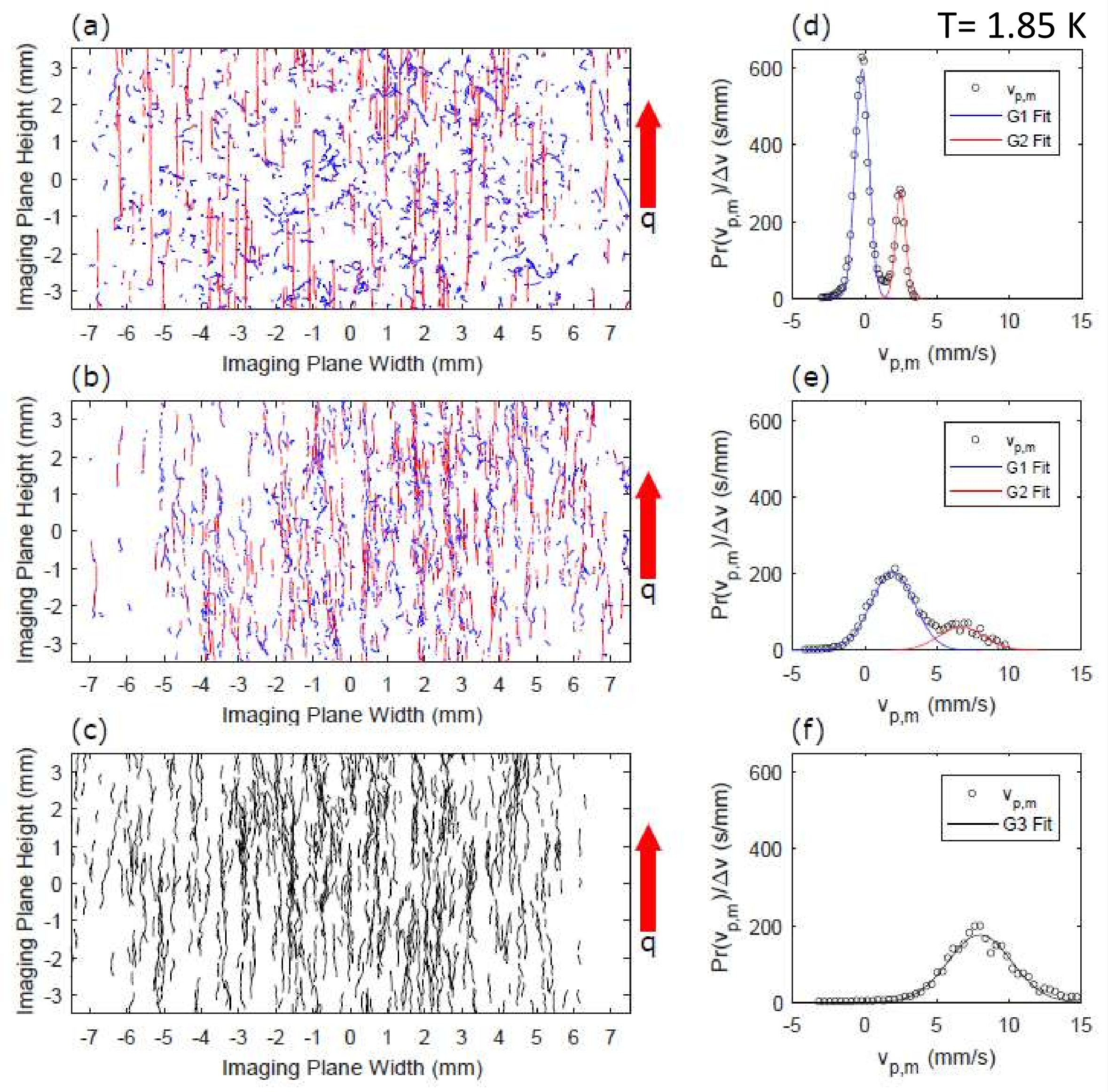

PIV/PTV techniques using micron-sized tracers

- Track length of the G2 particles → vortex spacing

Track length of G2 can be used to determine the mean free path, s, of the particles through the vortex tangle:

$$s \approx \frac{4}{\pi d_p L}$$

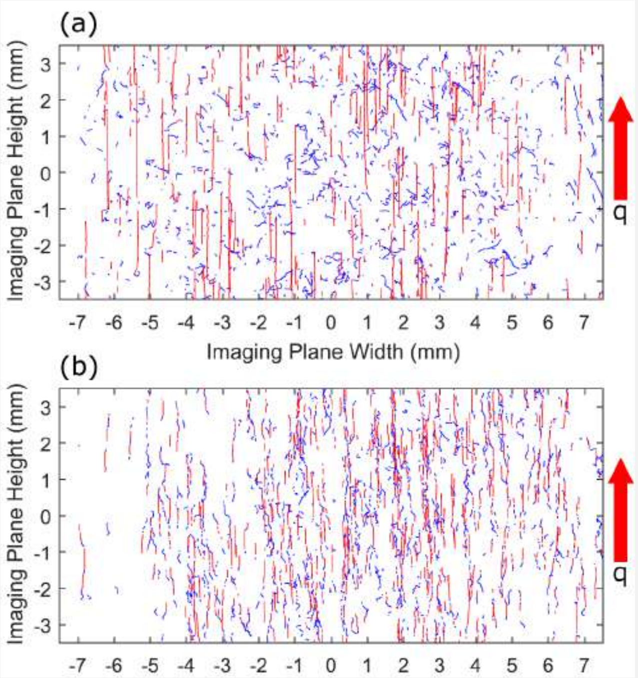

Result agrees very well with 2nd sound measurement

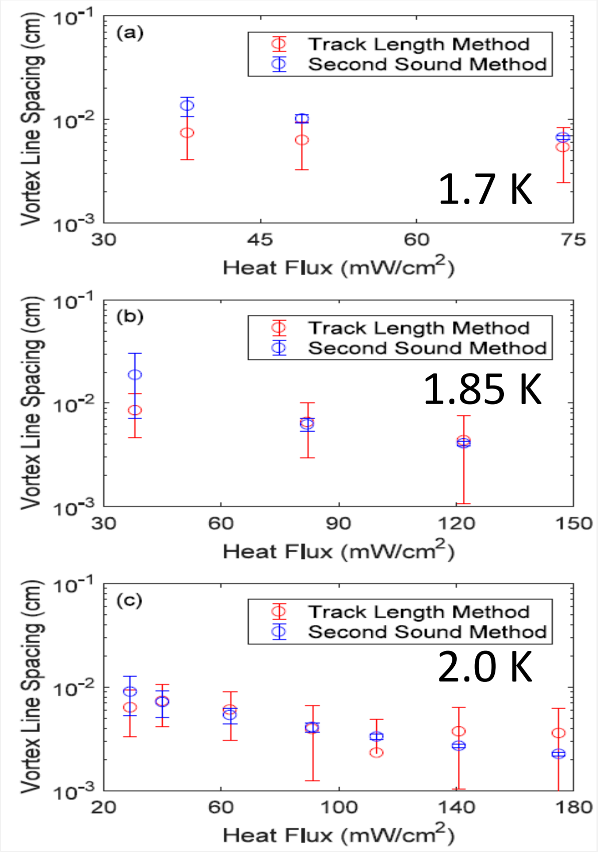

B. Mastracci and W. Guo, submitting to Phys. Rev. (2018)

2) PTV in grid turbulence:

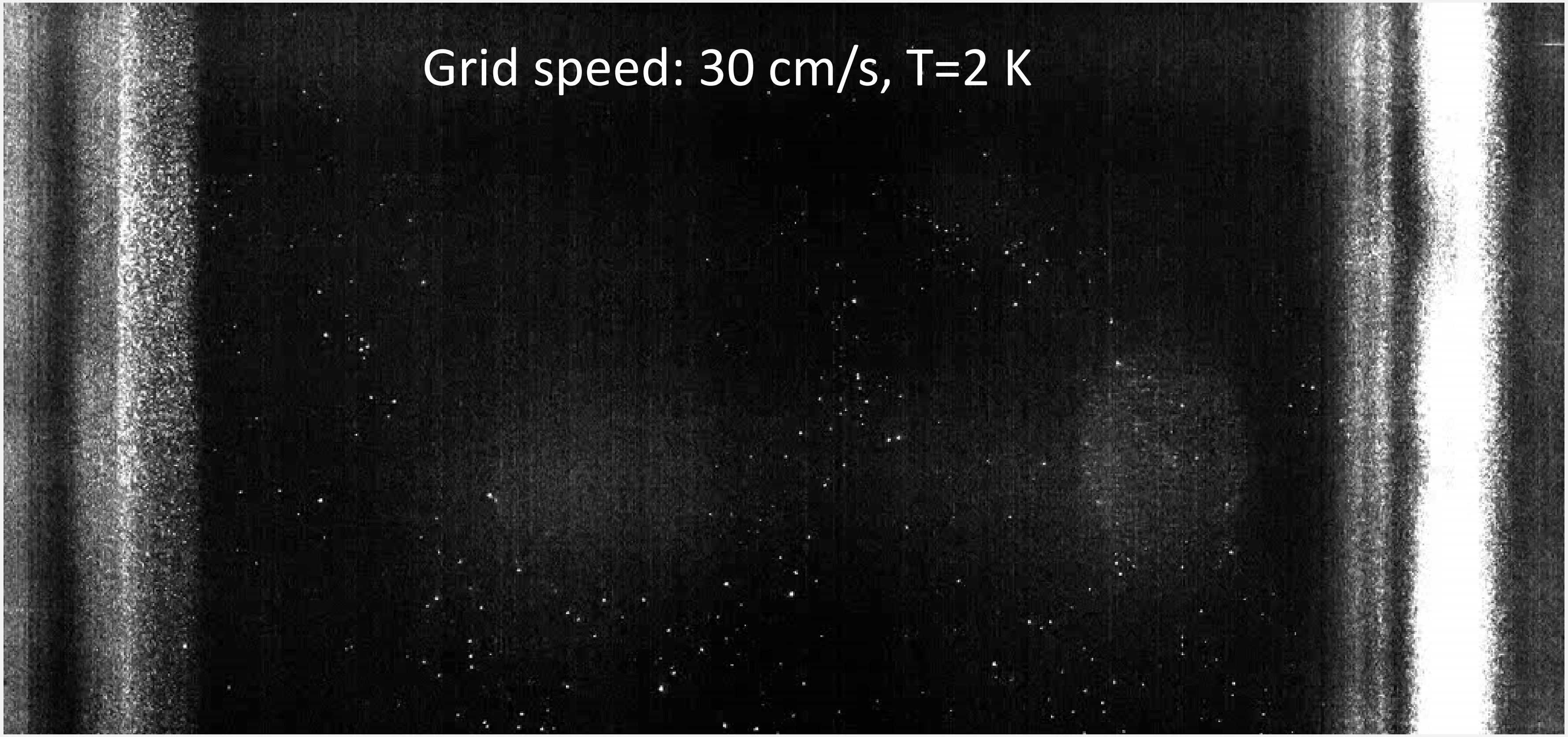

B. Mastracci and W. Guo, Rev. Sci. Instrum., 89, 015107 (2018)

- Particles are expected to trace the coupled flow in grid turbulence.

PIV/PTV techniques using micron-sized tracers

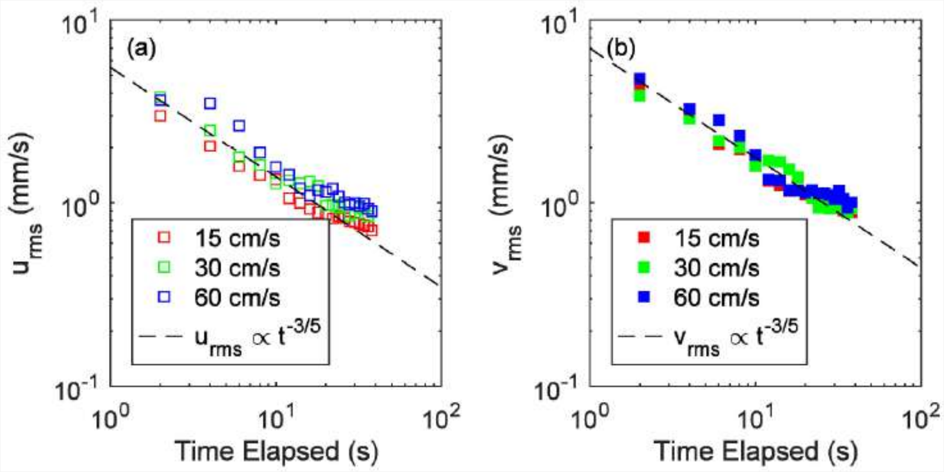

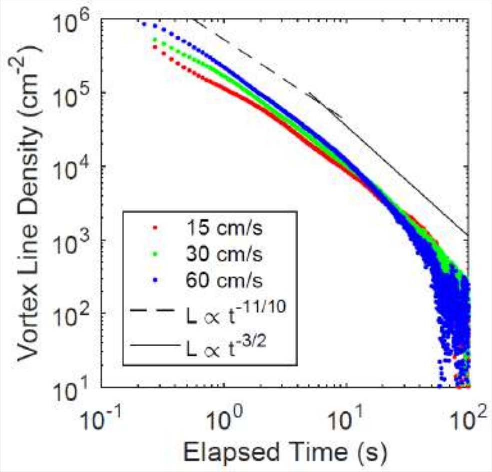

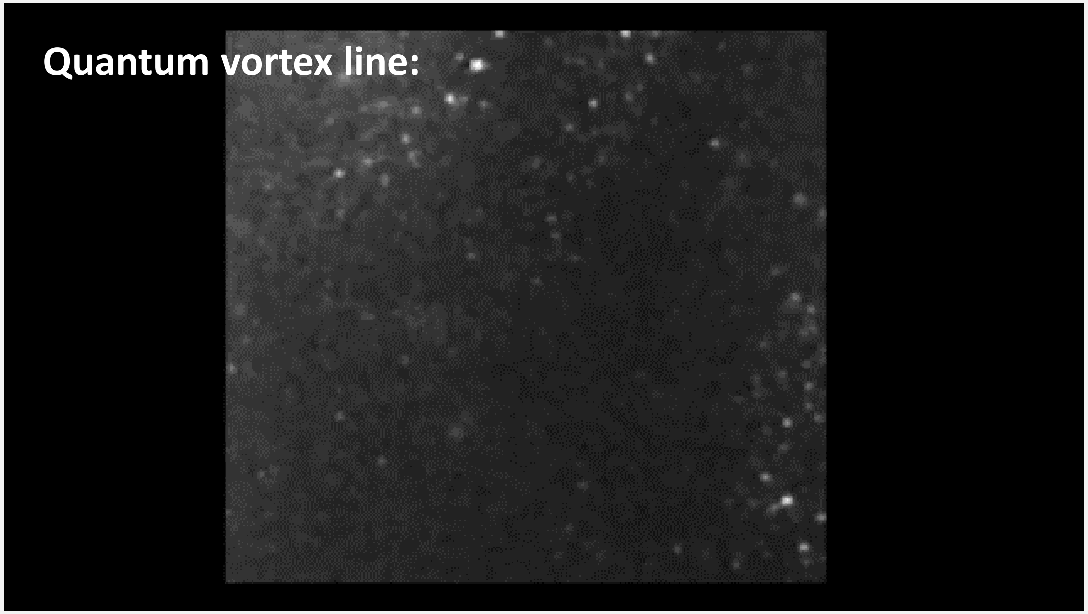

B. Mastracci and W. Guo, to be submitted to Phys. Rev. (2018)

MTV method using Metastable He_2^* excimer molecules

- Some issues of PIV/PTV method:

1. Particles have a wide size distribution and non-spherical shapes; they are not neutrally buoyant; they can form large clusters.

2. Particles interact with both the normal fluid and the vortices. Tracer behavior is hard to interpret.

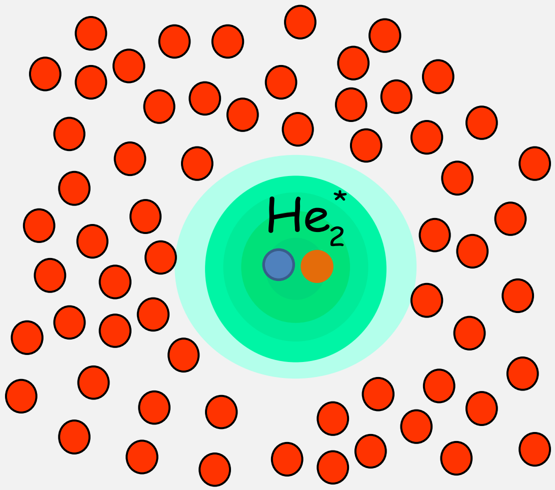

(D. Zmeev, et al, Phys. Rev. Lett., 110, 175303 (2013))

- Metastable He_2^* molecules can be easily produced as a result of ionization or excitation in LHe4:

$$e^- + He^+ + He \rightarrow He^* + He \rightarrow He^*_2$$

singlet state	$a^1\Sigma_u^+$	lifetime: ~1ns
triplet state	$a^3\Sigma_u^+$	lifetime: ~13s

- Above 1K : molecules trace the normal-fluid component only.
- Below 0.5 K : molecules can be trapped on vortex lines

Imaging He_2^* molecules: Laser-induced fluorescence

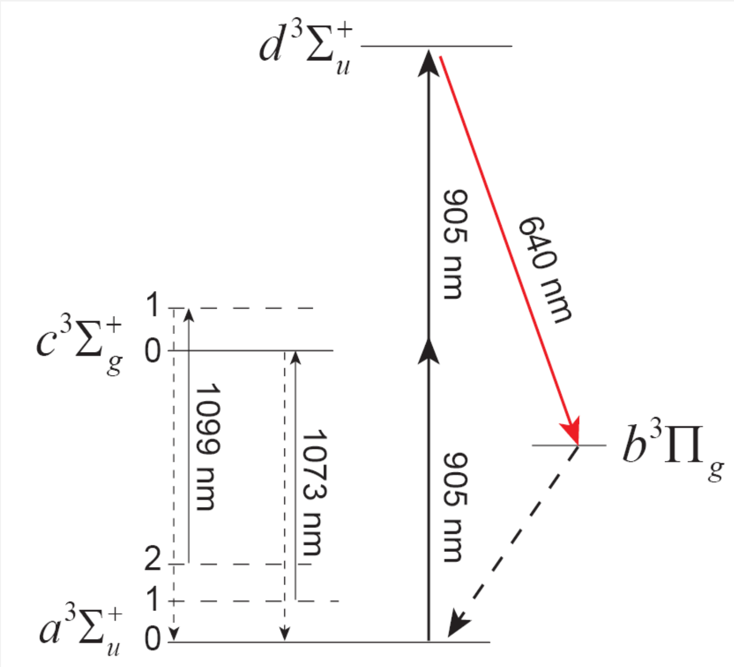

W.G. Rellergert *et al.*, Phys. Rev. Lett, 100 (2008).

For molecules in the triplet ground state a(0):

- A 905 nm pulsed laser is used to drive a cycling transition.
- Fluorescent light emitted at 640 nm.

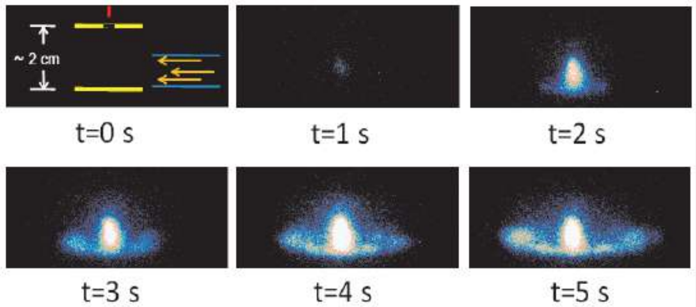

Guo, et al., J. Low Temp. Phys., 158, 346 (2009)

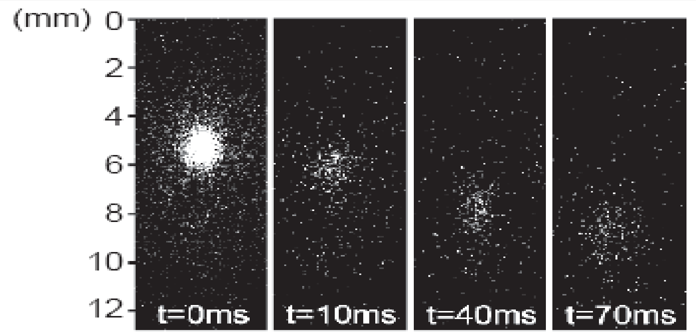

Guo, *et al.*, Phys. Rev. Lett., 102, 235301 (2009)

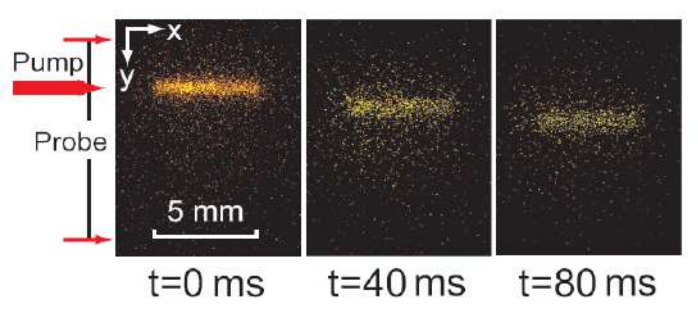

Guo, et al., Phys. Rev. Lett. 105, 045301 (2010).

Imaging He_2^* molecules: Laser-induced fluorescence

Femtosecond laser field ionization in helium:

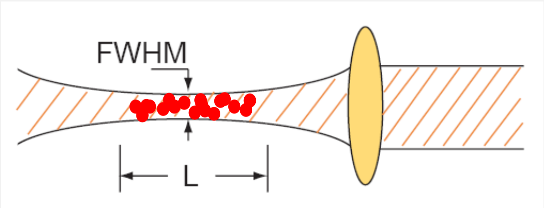

$I \geq 10^{13}\ \mathrm{W/cm^2}$

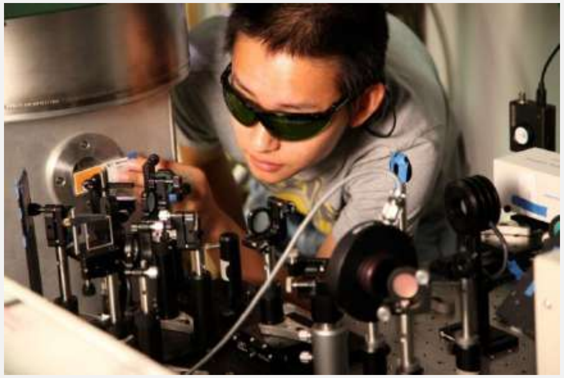

Pulse length: 35 fs

Pulse energy: up to 4 mJ

Rep rate: up to 5 kHz

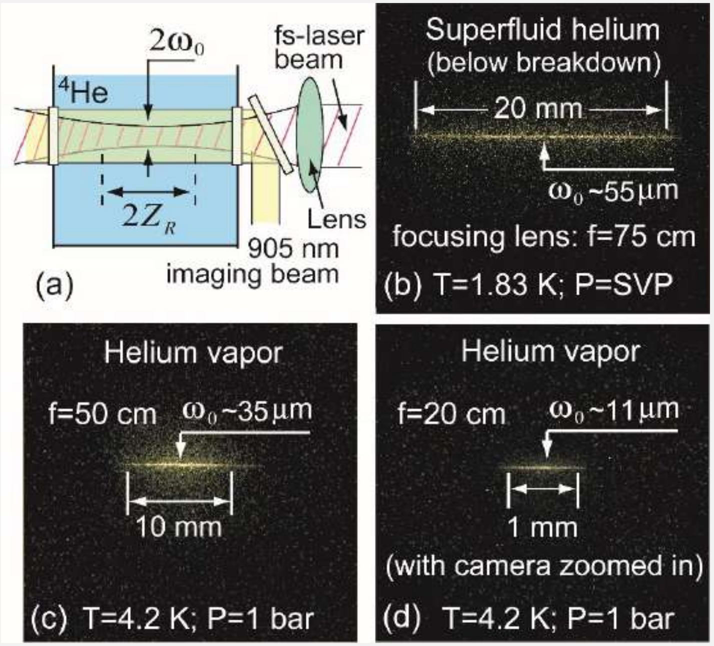

J. Gao, et al., Rev. Sci. Instrum. 86, 093904 (2015)

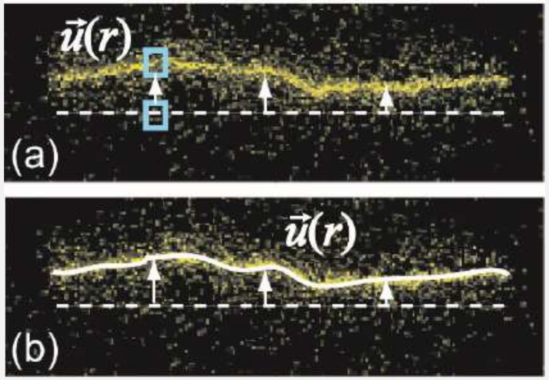

W. Guo, *et al.*, PNAS, 111, 4653 (2014)

- Thin tracer lines can be produced and tracked, allowing high precision flow field measurement.
- This technique is applicable to He II, He-I, and gaseous helium.

MTV study on steady counterflow in He II

- Three distinct velocity profiles of the normal fluid were observed.

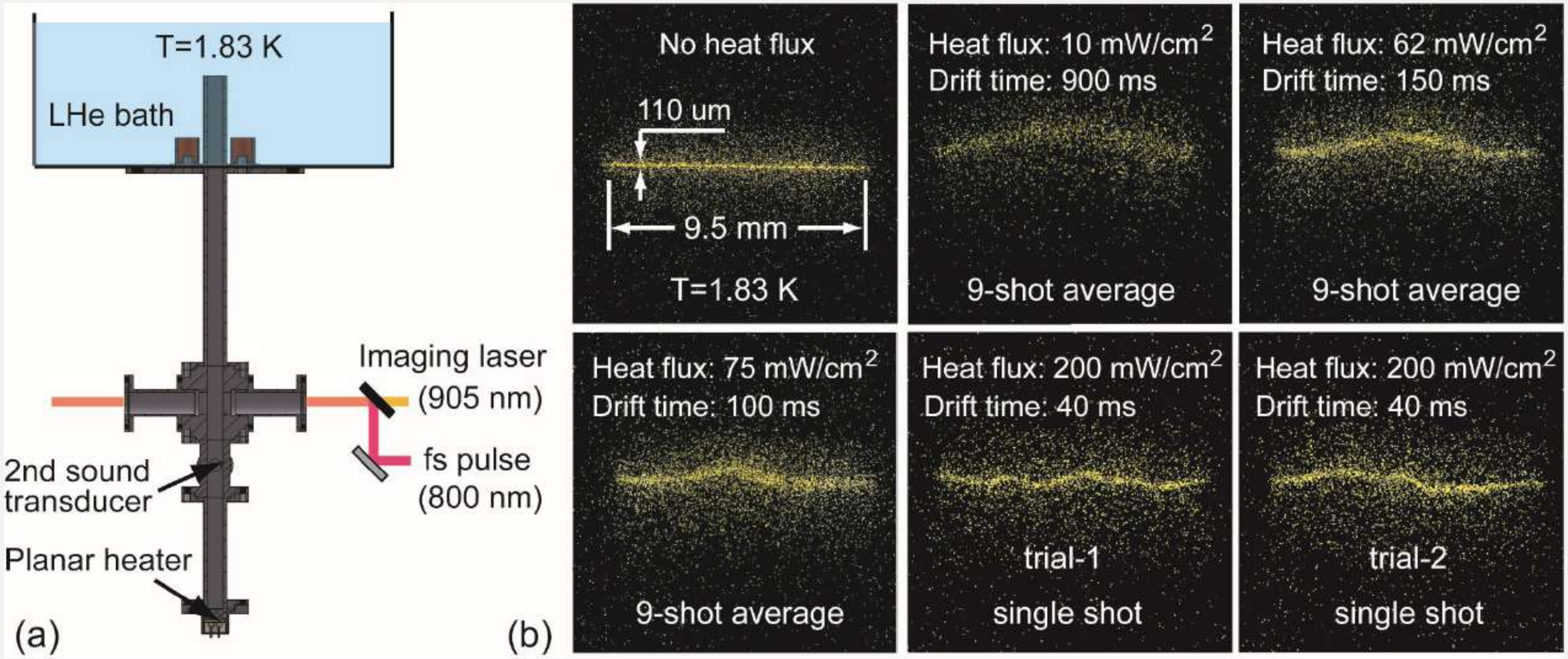

A. Marakov, G. Jian, et al., Phys. Rev. B 91, 094503 (2015).

- Recent simulations suggest that the mutual friction near the wall may flatten the profile of the normal fluid.

A. W. Baggaley and S. Laizet, Phys. Fluids 25, 115101 (2013)

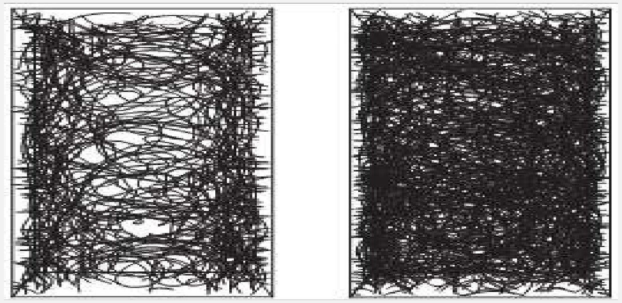

MTV study on steady counterflow in He II

- The velocity PDF in turbulent normal fluid is found to be a Gaussian. The turbulence intensity is higher than classical channel flow:

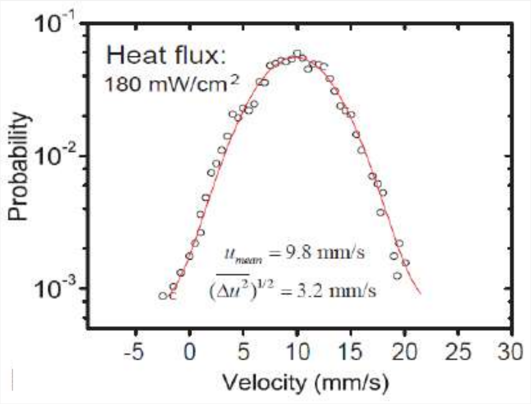

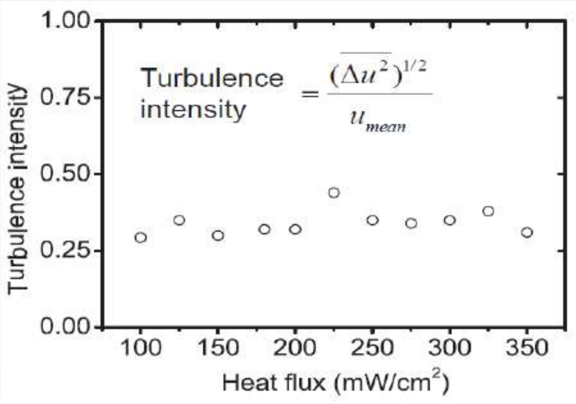

- The 2nd order transverse structure function revealed novel form of turbulence

$$S_2^{\perp}(R,r) = \overline{\langle (u(R+r) - u(R))^2 \rangle}$$

$$\boxed{S_2(r) \propto r^n \Longleftrightarrow E(k) \propto k^{-(n+1)}}$$

$$\Rightarrow \tilde{E}(k) \propto k^{-2}$$

S. Bao, W. Guo, et al., Phys. Rev. B 98, 174509 (2018).

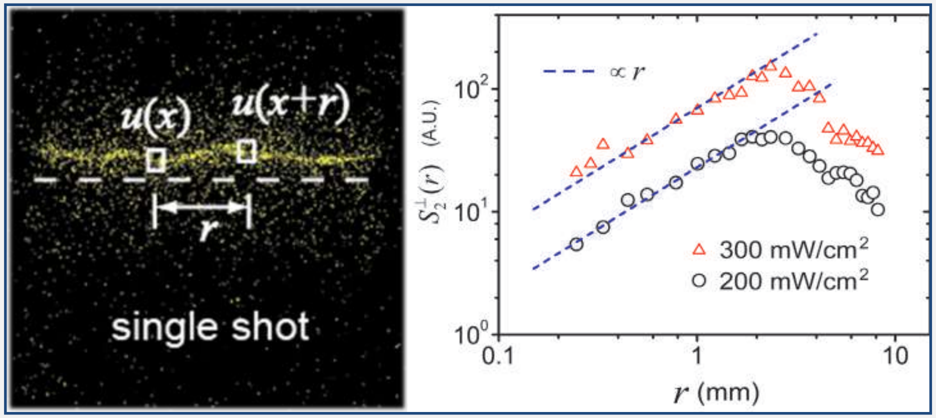

A. Marakov, J. Gao, et al., Phys. Rev. B 91, 094503 (2015).

③

Defects location on SRF cavities by MTV

Superconducting radio-frequency (SRF) cavities

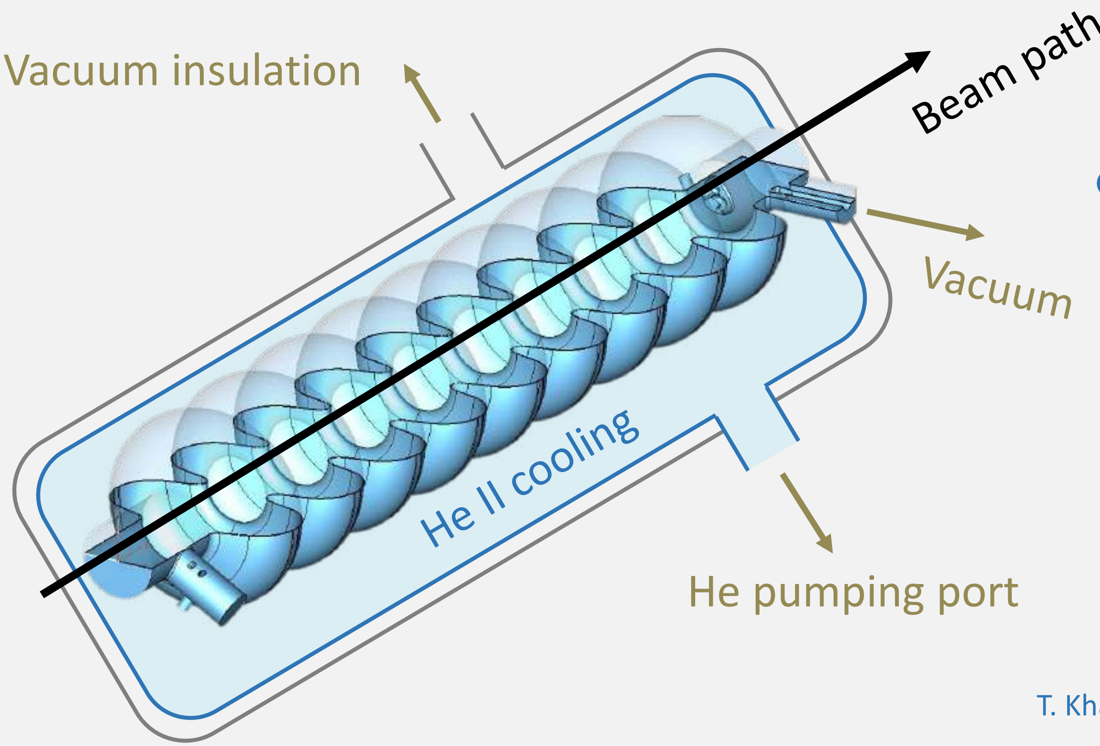

- SRF Cavities Applications:

  High Energy Physics: LHC, CEBAF;
  Radiation Sources: XFEL, ERL;
  Nuclear Physics: ATLAS, TRIUMF, SNS, EURSOL;
  Upcoming: ESS, FRIB, PIP-II …

T. Khabiboulline, Engineering for Particle Accelerators, (2017).

- SRF cavities are key components in many modern particle accelerators due to their high Q factors.
- The maximum acceleration gradient is limited by the 'quench' of SRF cavities.

③ Superconducting RF cavities and surface quench spots

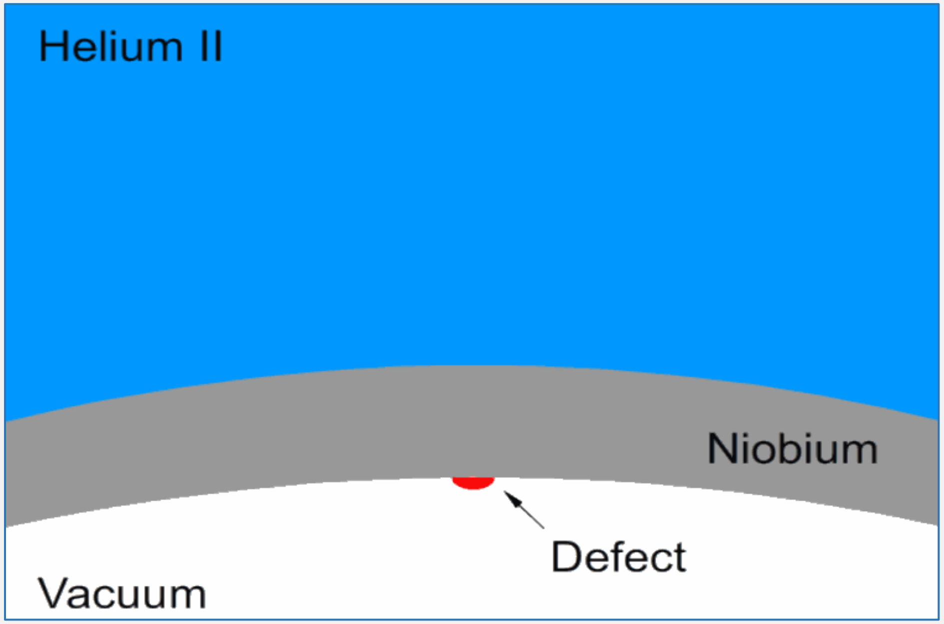

- The quenching spot causes transient heat transfer into He II (≈1 ms, 1-10 J).
- The maximum achievable field can be improved by removing the surface defects by mechanical grinding, tumbling the cavity, and electron or laser re-melting.
- Precise location of the hotspots is prerequisite for a successful repair.

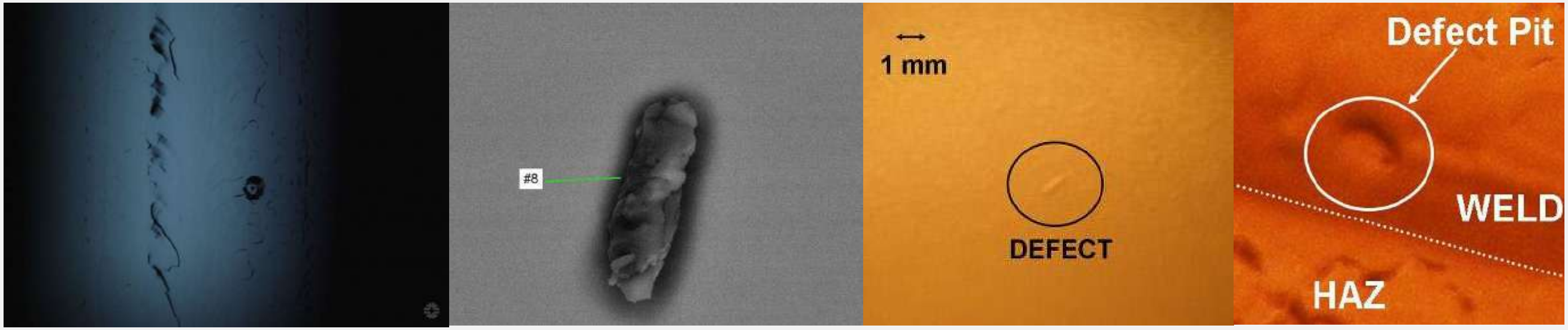

Typical defects images captured by Cornell University and DESY

Existing methods: (1). Temperature mapping

Surface T-mapping

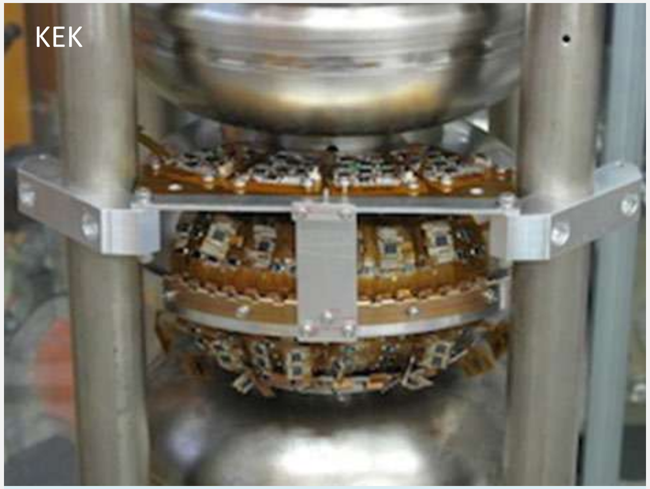

- Installation and maintenance required for over 1000 temperature sensors and wires.

Rotational T-mapping

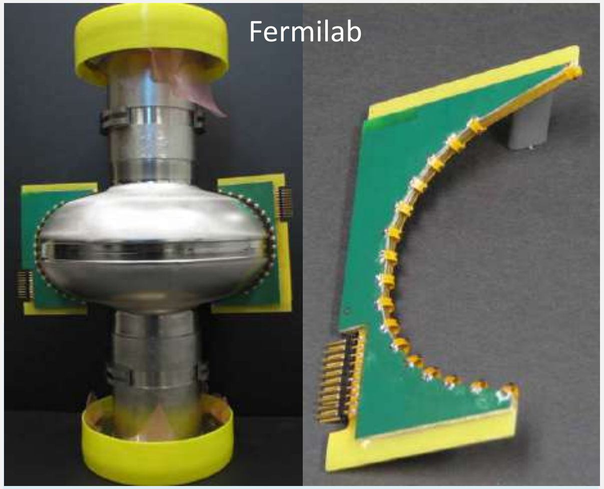

- Low sensitivity due to the gap between the sensor and cavity surface.

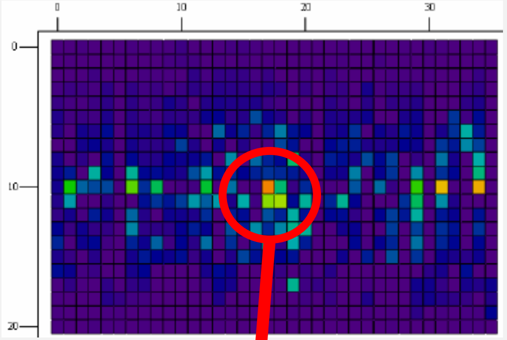

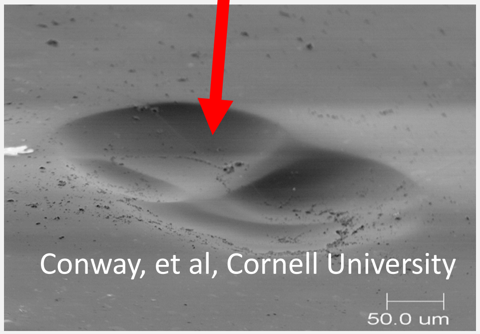

- Conducted just below the quench threshold. At least 2 cool downs and reconfiguration of the sensor are normally needed for good accuracy

Existing methods: (2). 2nd sound trilateration

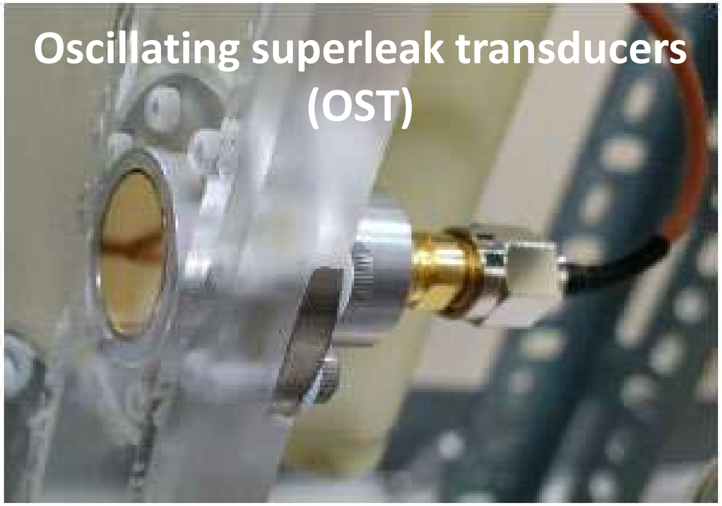

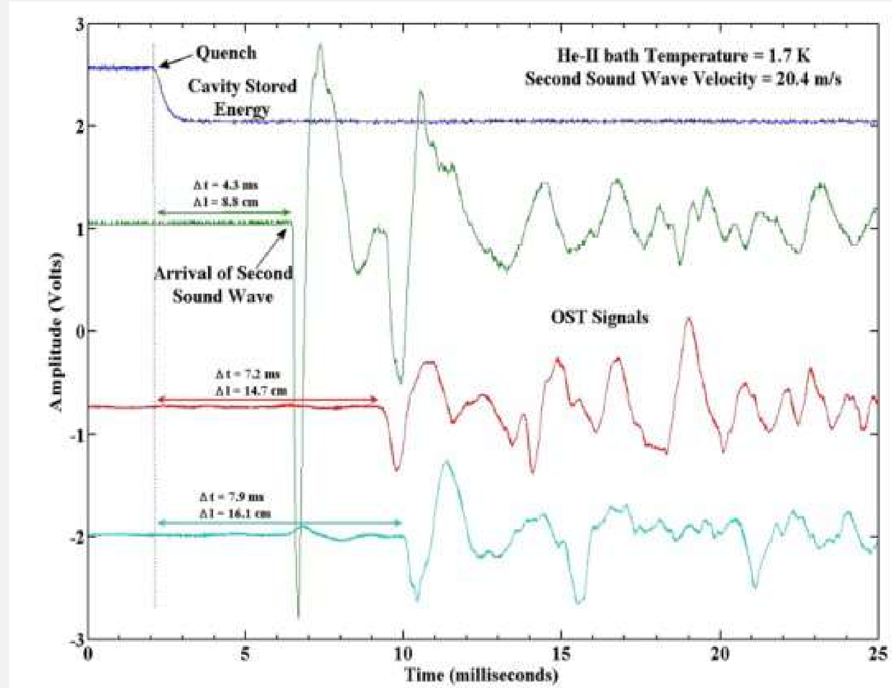

Conway, et al., Supercond. Sci. Technol. 30, 034002 (2017).

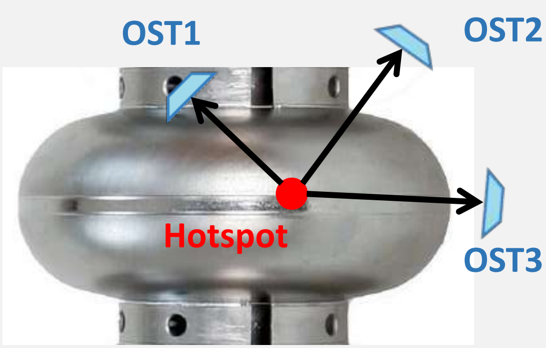

- Hotspot leads to emission of 2nd sound waves in He II.
- Converged location can have an uncertainty of 5-10 mm.
- Convergence of the signals requires a 2nd sound speed different than known value.

Possible non-contacting detection via flow visualization

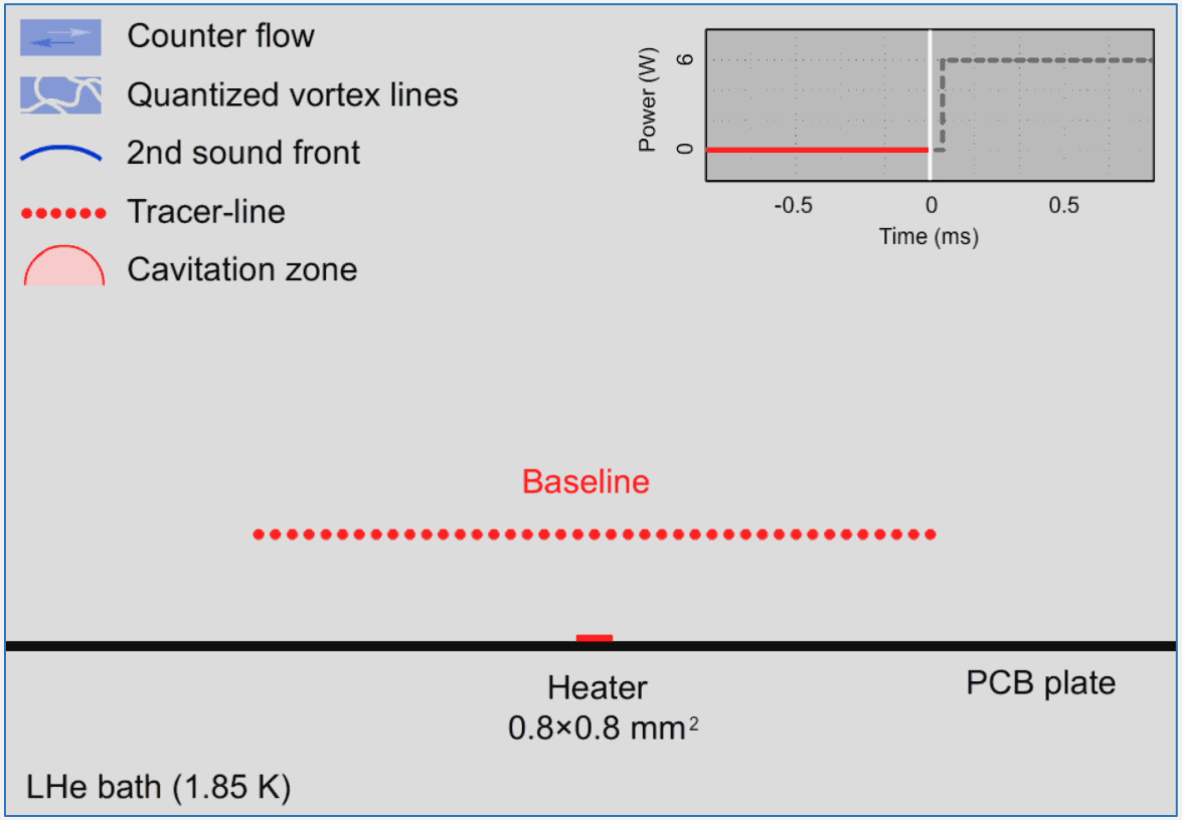

Heat transfer & flow process following a transient point-like heat pulse

- Accurate non-contacting detection by flow visualization in He II

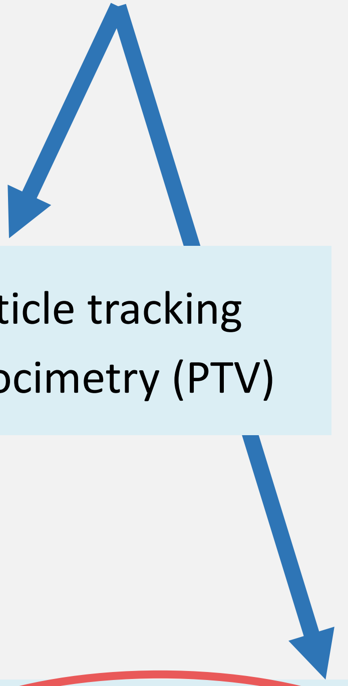

- Particle tracking velocimetry (PTV)
- Molecular tagging velocimetry (MTV)

- A heat-induced counterflow carries detailed information of the heating source: amplitude, duration, size…

Proof-of-concept experiment using SMD heaters

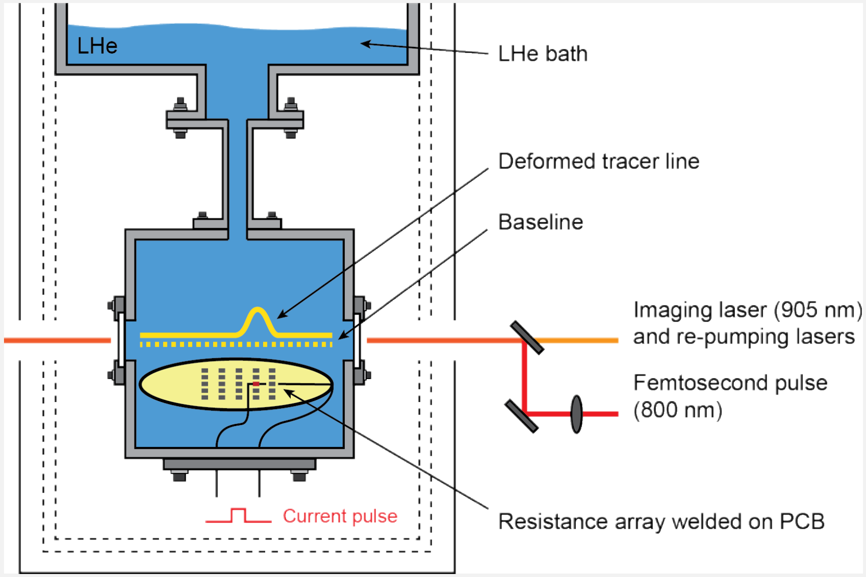

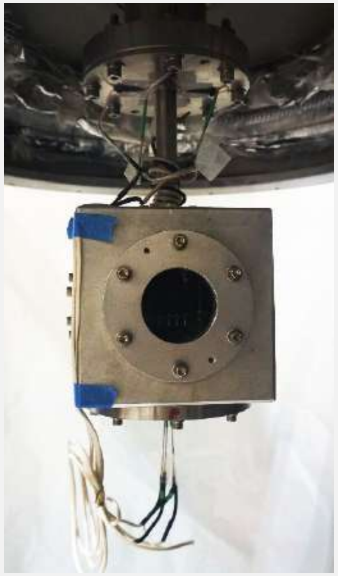

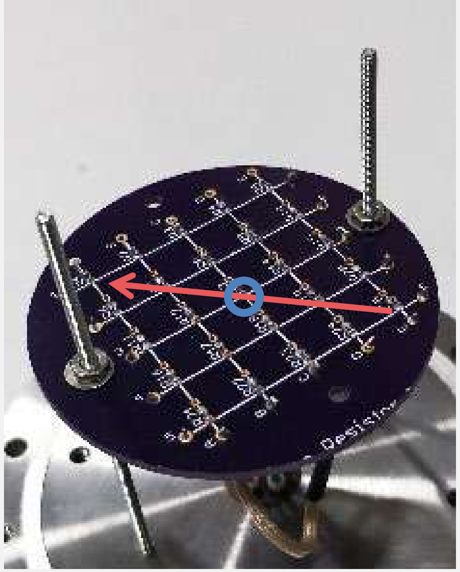

- An array of thin film resistors (50 Ohm, 0.8x0.8 mm^2).
- The PCB is in He II at controlled temperatures (1.85 K).
- A voltage pulse (1-8 ms) is applied to a chosen heater (78-287 W/cm^2).

S. Bao and W. Guo, arXiv:1812.07080 (2018)
(submitting to Phys. Rev. Applied)

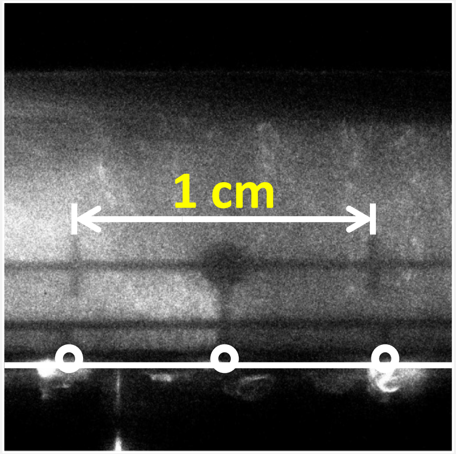

Typical baseline and deformed tracer-line images

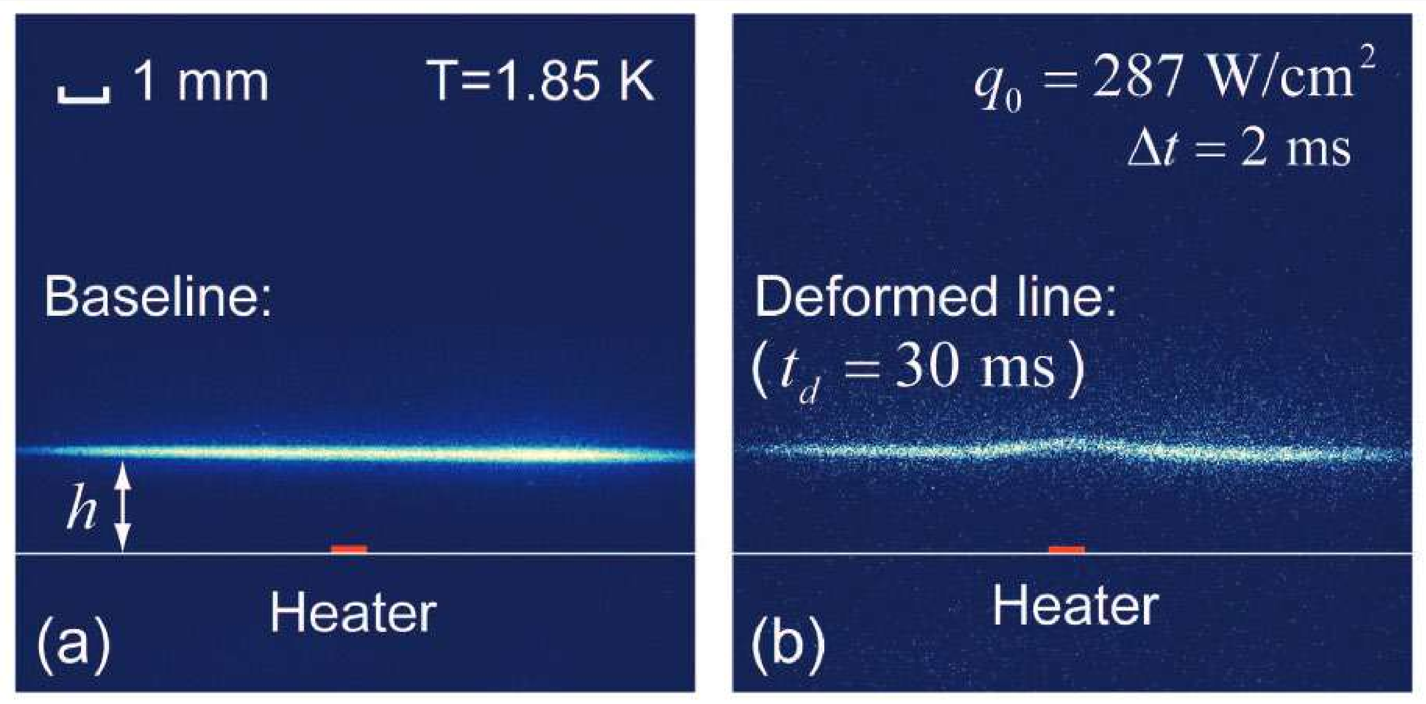

$$dr = v_n \cdot dt = \frac{q(r)}{\rho s T} \cdot dt$$

$$r_f^3 = r_0^3 + \frac{3}{2\pi\rho s T}\int_{t_0}^{t_0+\Delta t} \dot{Q}_s dt = r_0^3 + \frac{3Q_s}{2\pi\rho s T}$$

- Two fitting parameters:
  1) The location of the heater: x_0 2) The total energy carried by second-sound: Q_s

Fitting results of the heater location

- The obtained x_0 is always within a few hundred microns from the actual heater location, clearly proves the feasibility of this novel technology.

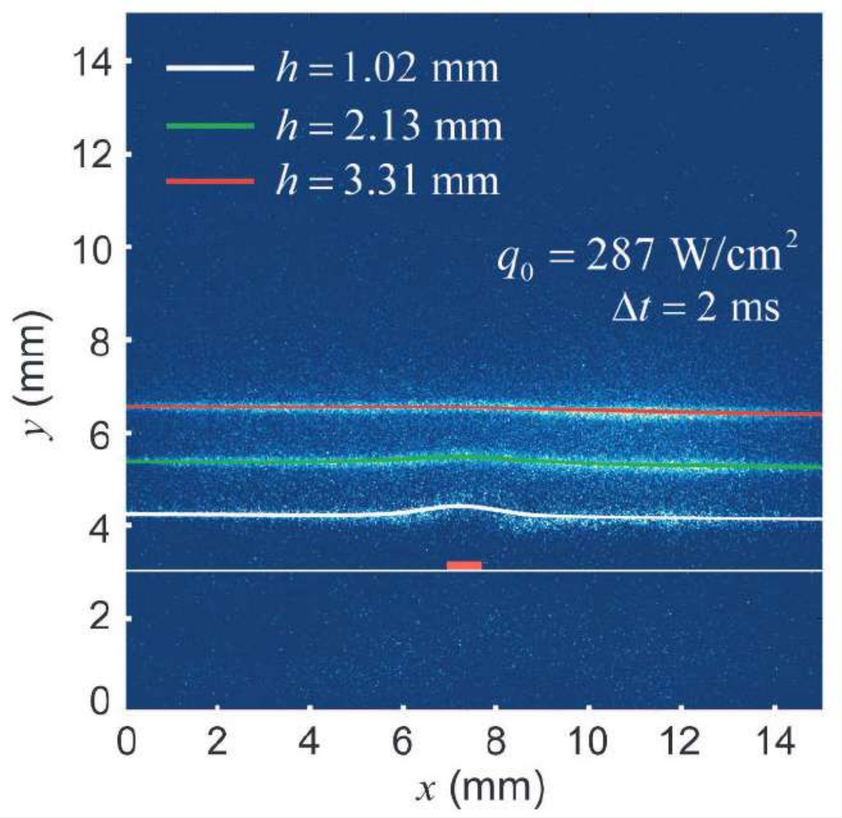

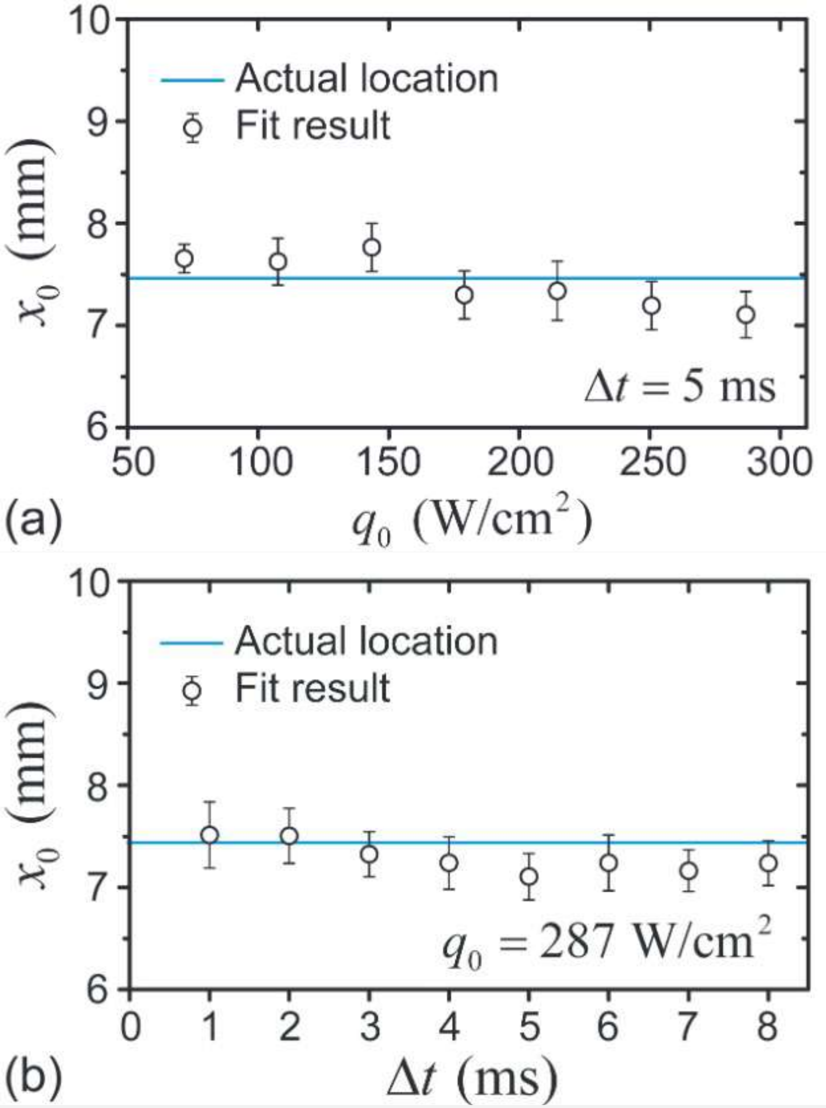

Possible origin of the "fast" second sound

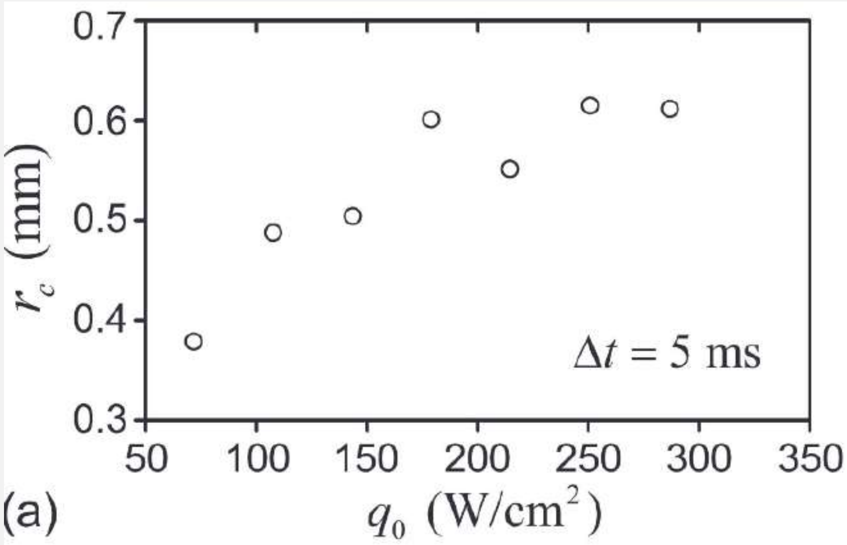

- The size of this cavitation zone is estimated based on the knowledge obtained about the transported heat. (15 W/cm^2 threshold is selected)

- A new explanation for the decades-long puzzle observed in previous second-sound triangulation experiments is proposed.

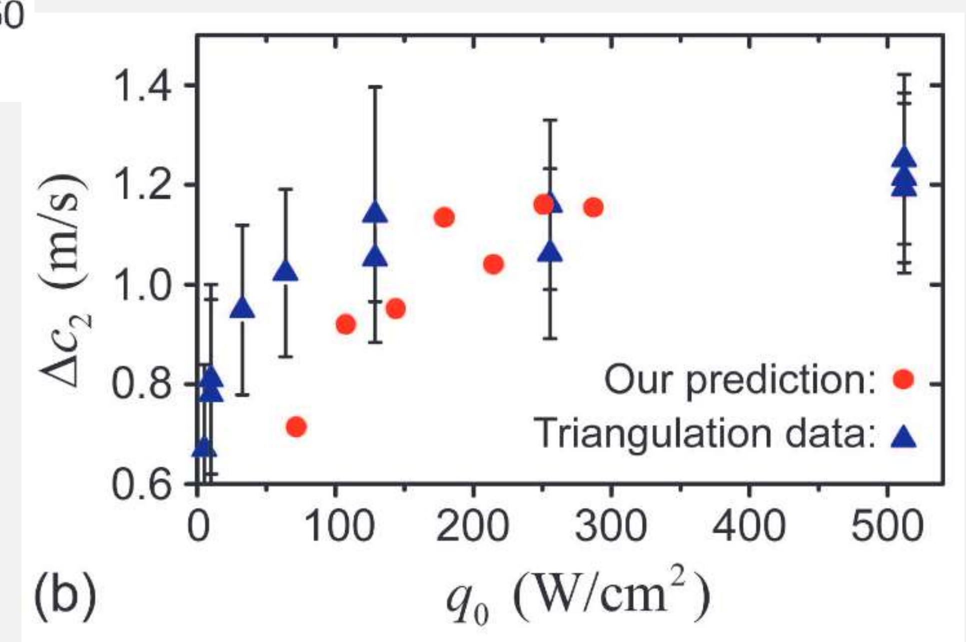

3D imaging of tracer-lines and quench spot detection

Our long-term goal:

Rotational quick scan of real cavities

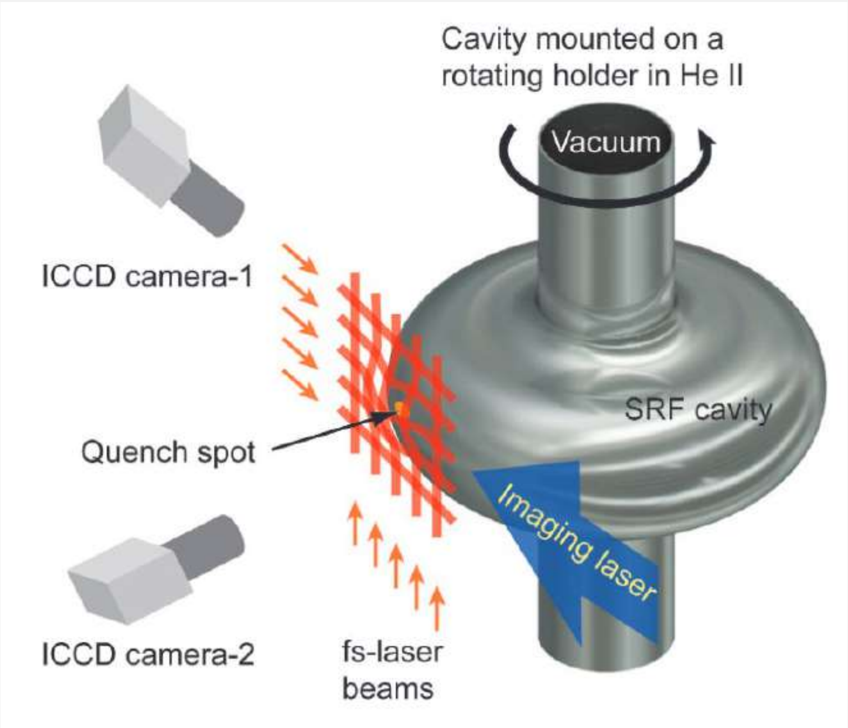

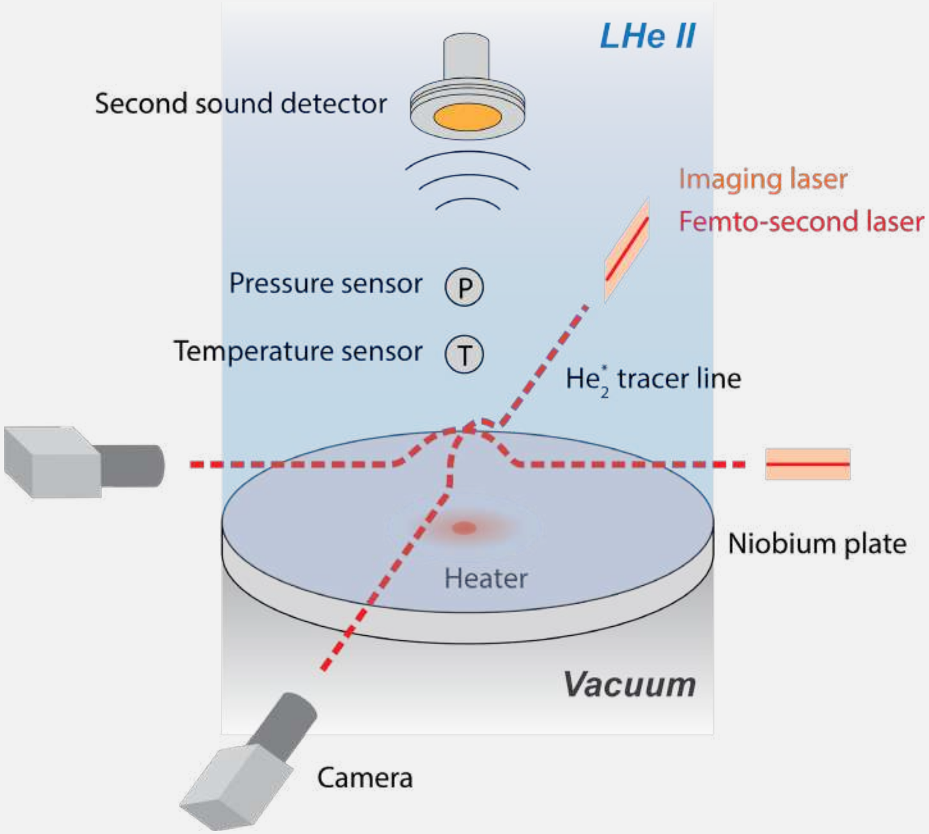

Test experiment:

3D imaging of 2 tracer-lines

3D imaging: Stereoscopic MTV experimental setup

- We built up a stereoscopic MTV system to capture the 3D profile of the tracer line for detecting a hot spot on a 2D surface.

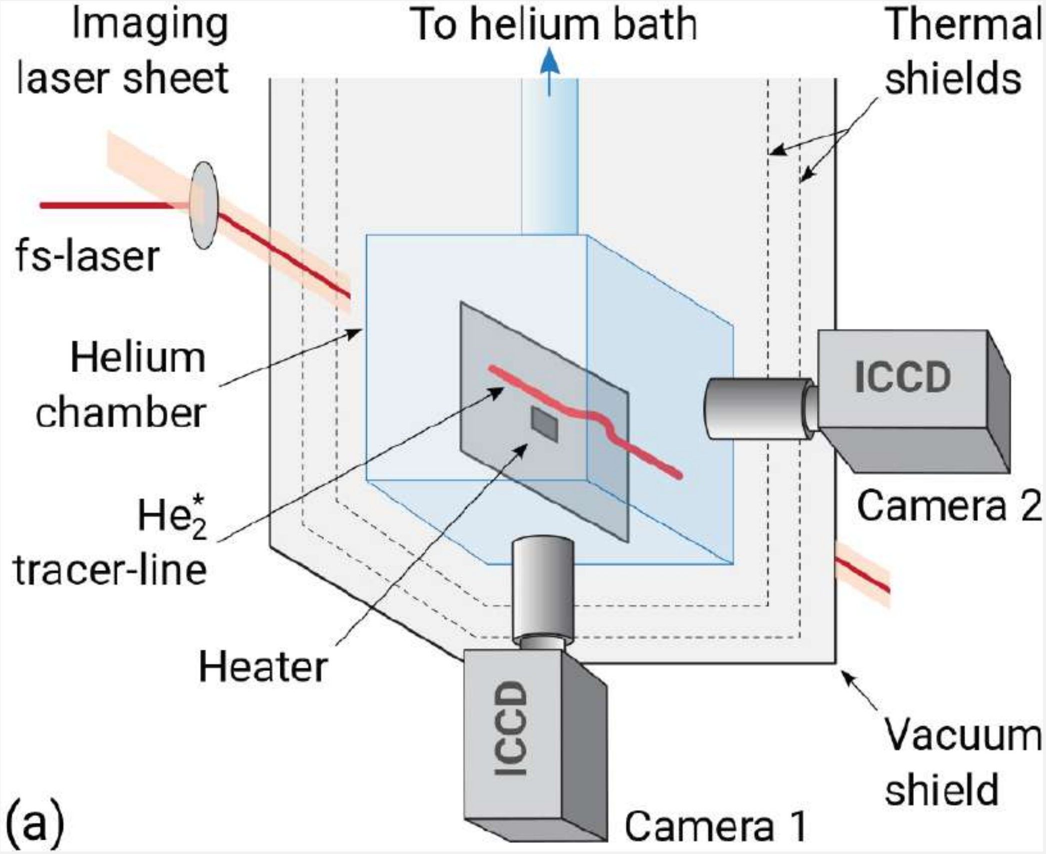

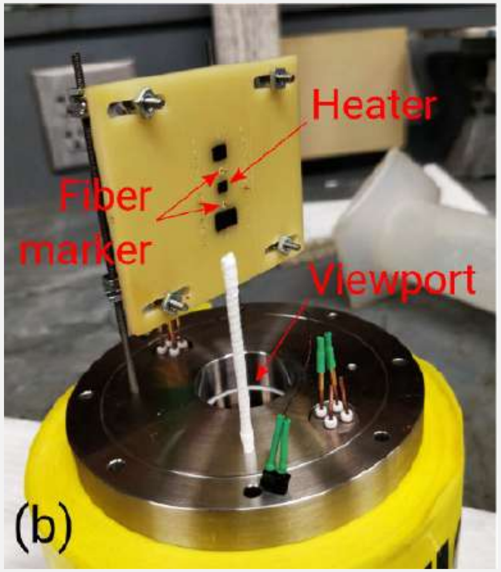

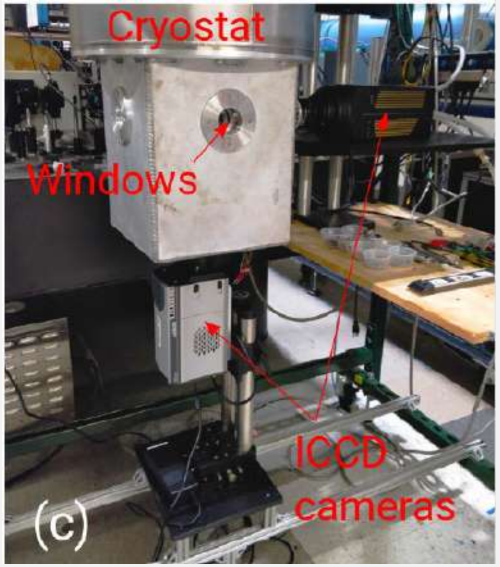

S.R. Bao and W. Guo, Int. J. Heat Mass Transf., 161, 120259 (2020).

3D imaging: Reconstruction of the tracer-line profile

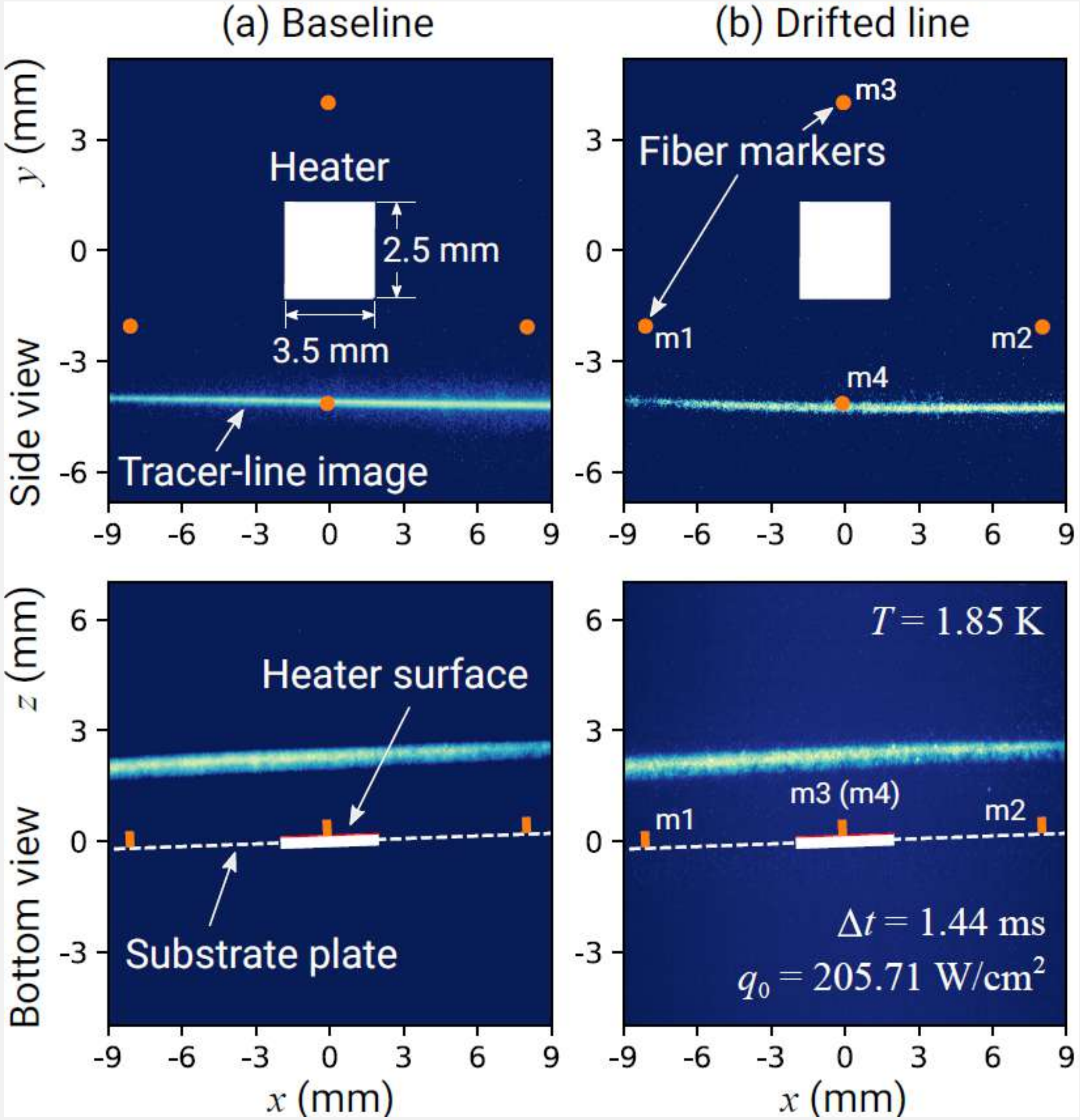

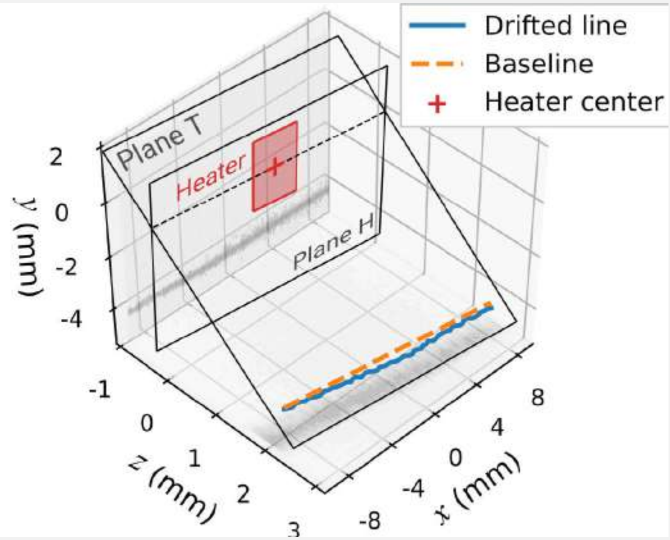

- Tracer line is created at about 4-5 mm away from the heater center.
- Reconstruction is performed based on the marker positions.

Simplified model based on the discretization of heater

- In the current experiment the heater size is increased by nearly nine times in order to better represent a quench spot, which makes the point heat-source model inapplicable.

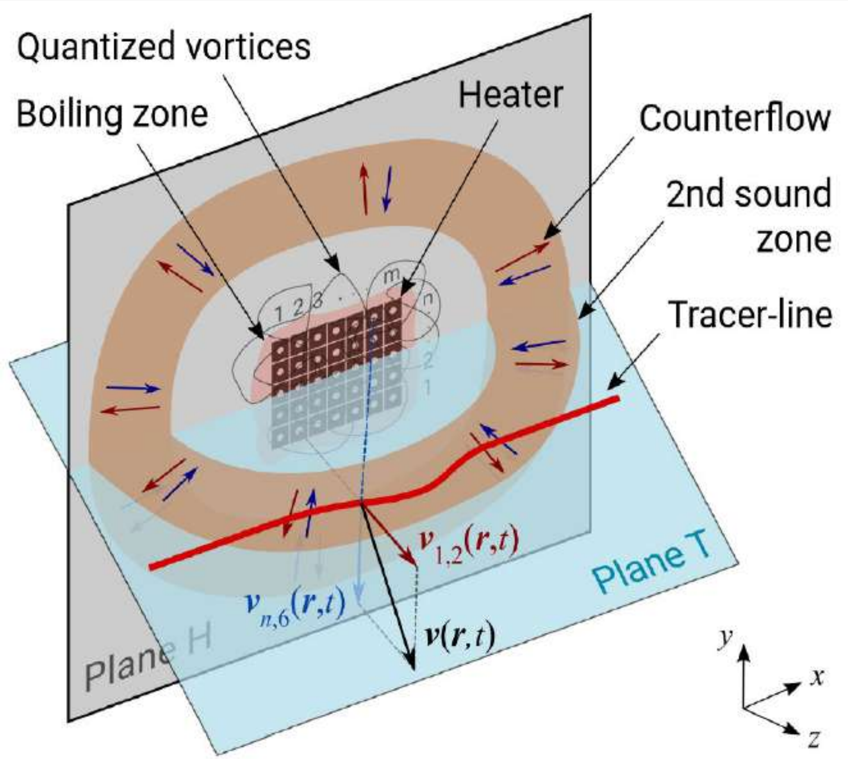

- We divide the assumed heater into n×m small elements and treat each element as a standalone point heat source. The velocity of a tracer-line segment located at ***r*** :

$$v(\mathbf{r},t)=\sum_{i=1}^{n}\sum_{j=1}^{m}v_{i,j}(\mathbf{r},t)=\sum_{i=1}^{n}\sum_{j=1}^{m}\frac{\mathbf{q}_{i,j}(t)}{\rho sT}$$

$$q_{i,j}(t)=\dot{Q}_{i,j}(t)/2\pi R_{i,j}^2 \qquad R_{i,j}=|\mathbf{r}_{i,j}-\mathbf{r}|$$

- The heat transfer rate is given by:

$$\dot{Q}_{i,j}(t)=\begin{cases}0 & c_2t<R_{i,j}\\ \frac{Q_s/\Delta t}{n\times m} & R_{i,j}\le c_2t\le R_{i,j}+c_2\Delta t\\ 0 & c_2t>R_{i,j}+c_2\Delta t\end{cases}$$

Simplified model based on the discretization of heater

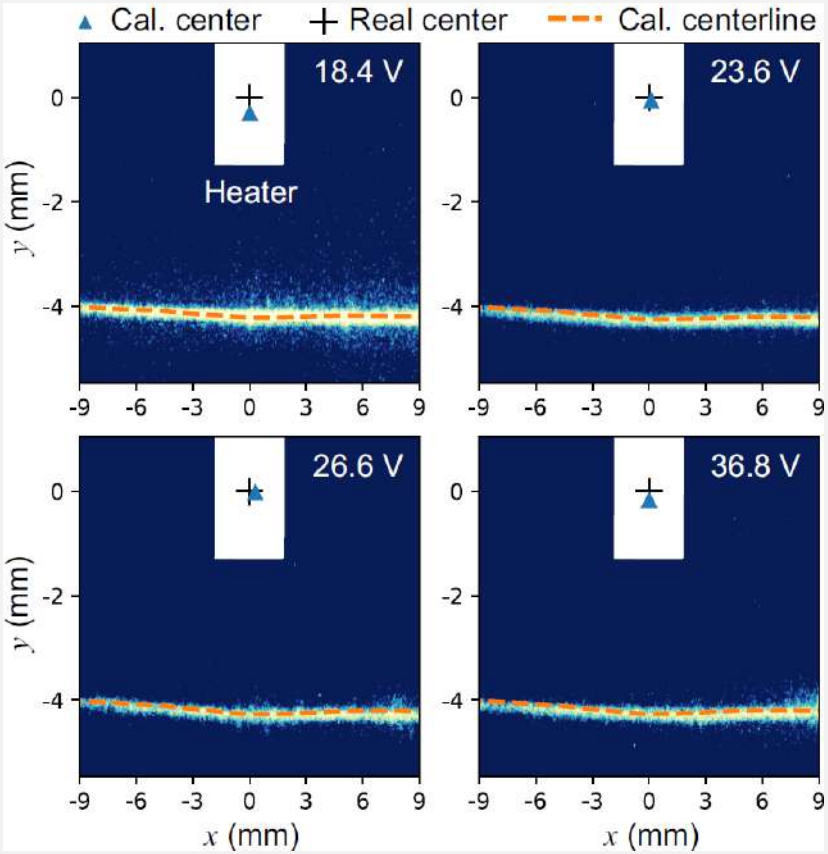

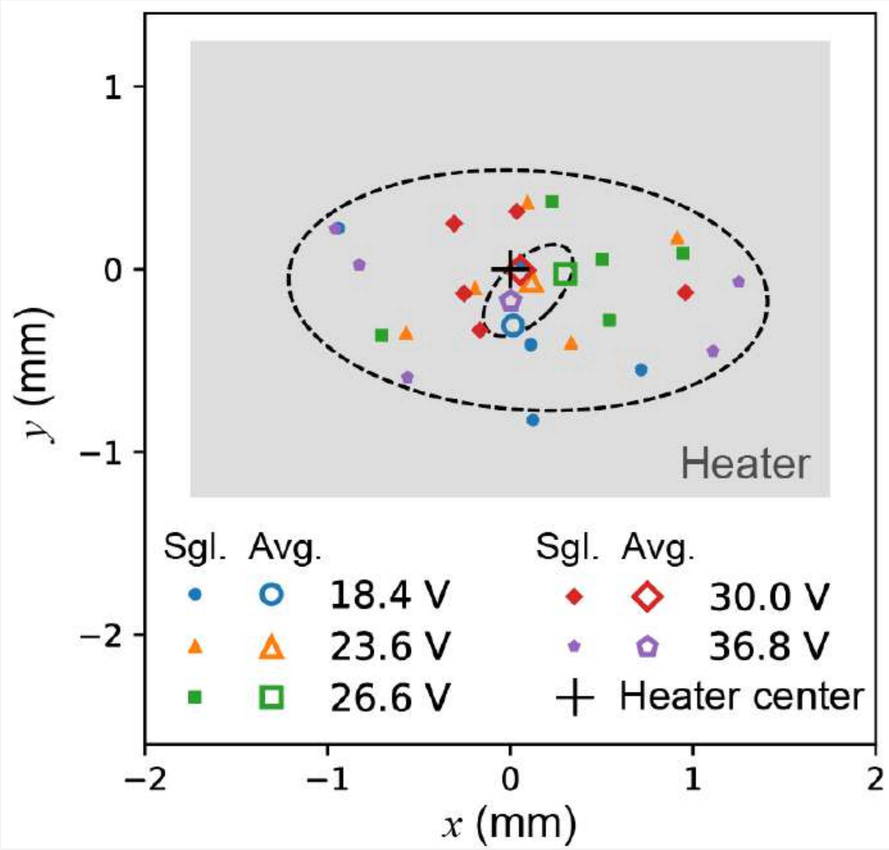

- Our analysis nicely reproduces the heater center with an uncertainty of a few hundred microns (a few percent of the heater size), regardless of the applied heat fluxes.

④

Vacuum loss in LHe cooled tube

Particle accelerators composed of LHe cooled cryomodules

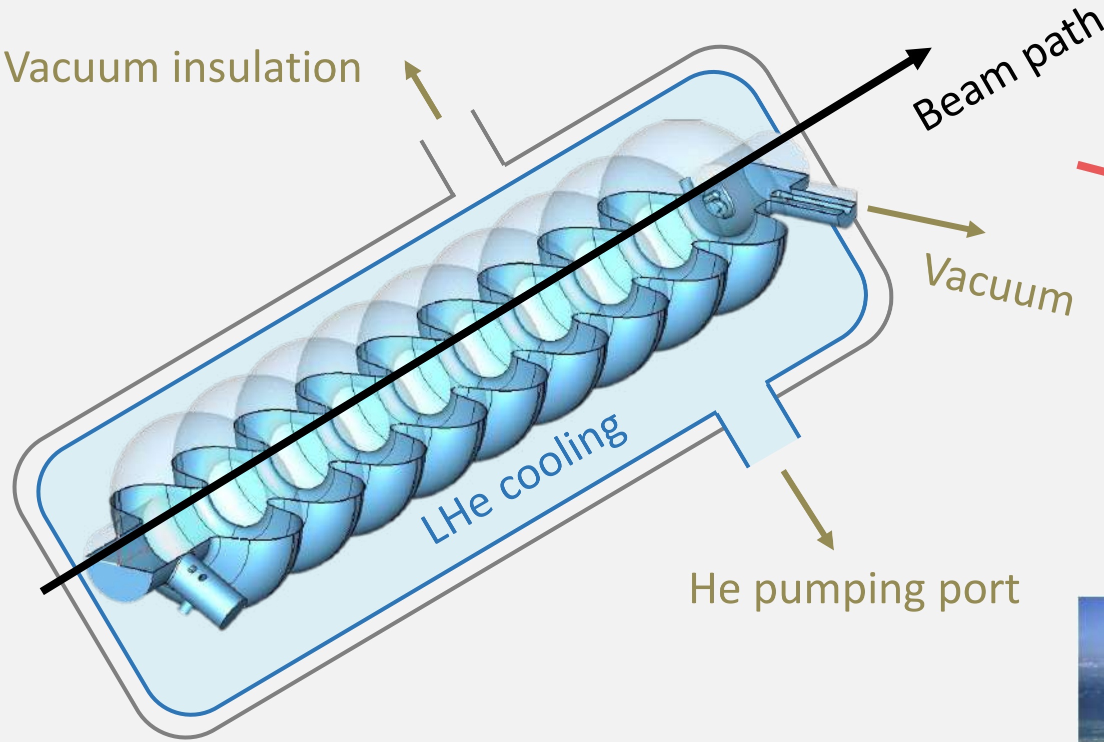

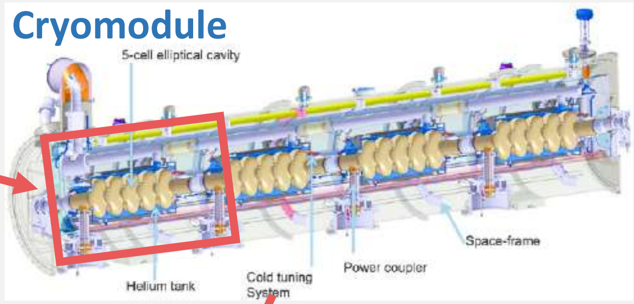

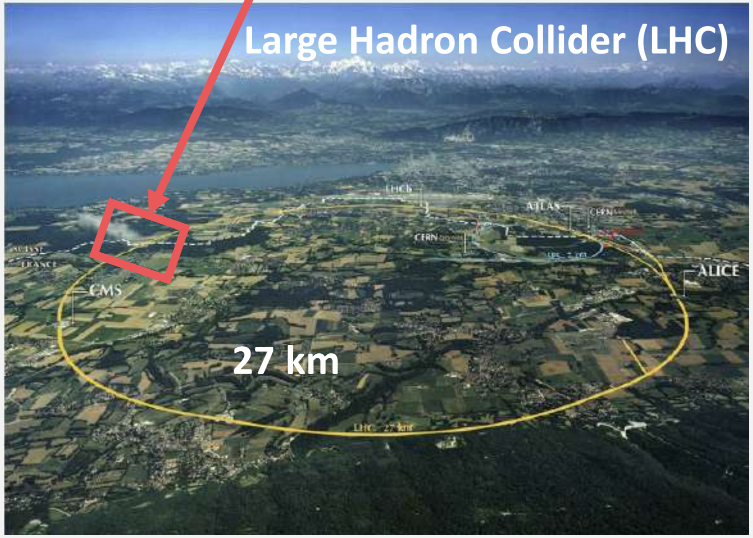

Vacuum break in large-scale particle-accelerator

- A sudden catastrophic loss of vacuum is one of the most serious failures in LHe cooled particle-accelerator systems

Insulation vacuum space

(usually isolated per cryomodule)

- Loss of vacuum insulation leads to explosive boiloff
- Equipment damage
- Personnel injury
- Oxygen deficiency

Vacuum beamline

(interconnected to create a beamline up to kilometers)

- Gas propagating in the beam tube could affect the entire system
- Introduce contamination to the inner surface of cavities

- Example: LHC, CERN 2008
  - Beam tube vacuum failure
  - 53 cryomodules contaminated/damaged
  - 6 tons helium lost
  - 6 months to repair

Developing a **clear understanding of the complex dynamical heat and mass transfer processes** involved following a sudden vacuum break is of great importance for the safe operation of accelerators.

Early experiments in a straight tube immersed in He I

- Early experiments conducted in straight tube immersed in He I by Dhuley and Van Sciver in our lab confirmed the slowing down propagation

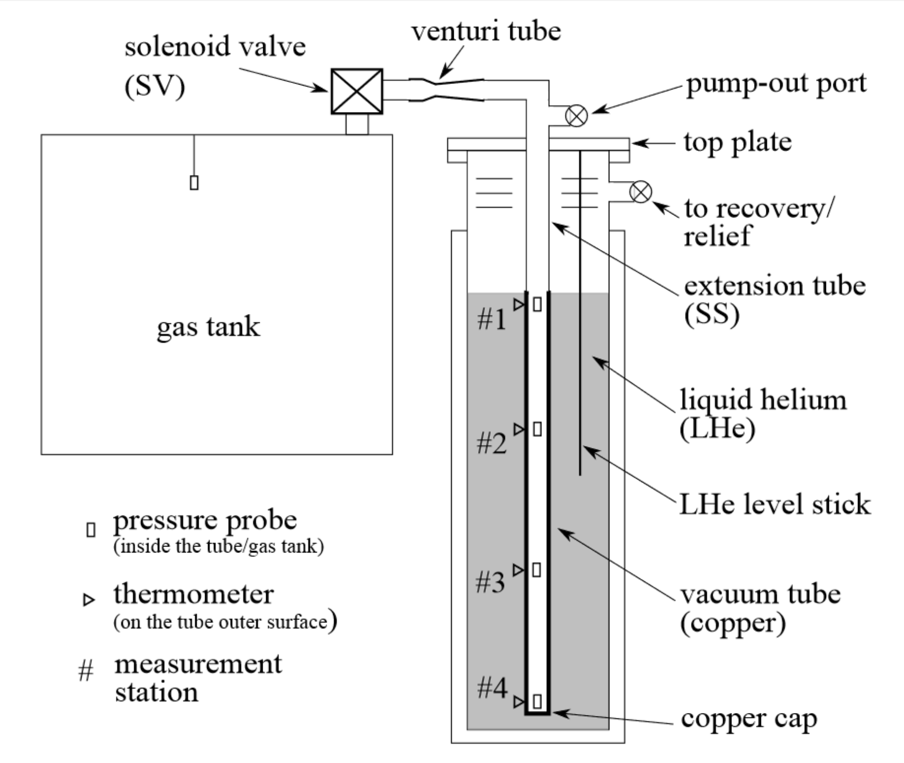

Length: **1.5 m**; Inner diameter: 32 mm

How to measure the gas front in cryogenic temperature?

Pressure Sensor

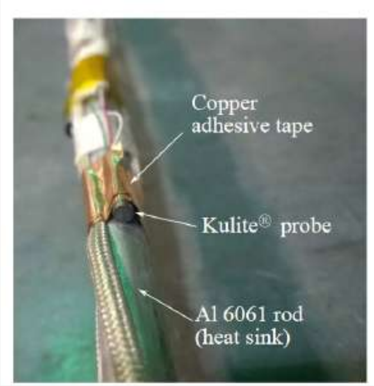

Temperature Sensor

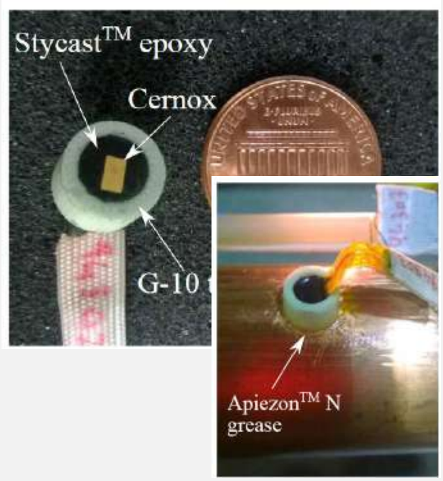

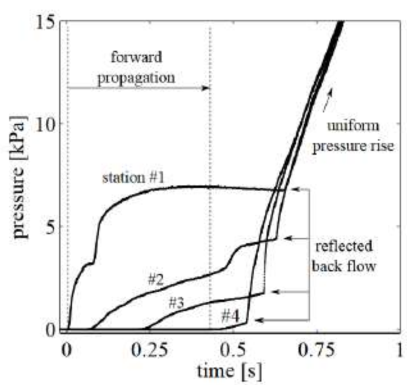

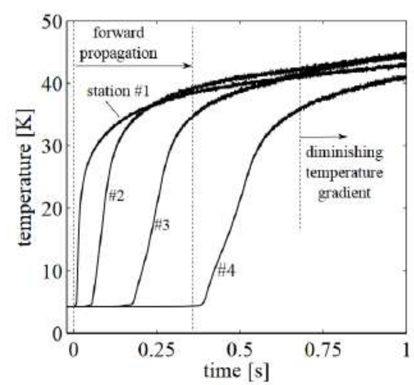

④ Early experiments in a straight tube immersed in He I

- Dhuley and Van Sciver attributed the exponential slowing of the gas front propagation to gas condensing and freezing to the walls. They proposed a simple model based on conservation of mass analysis in one dimensional tube flow.

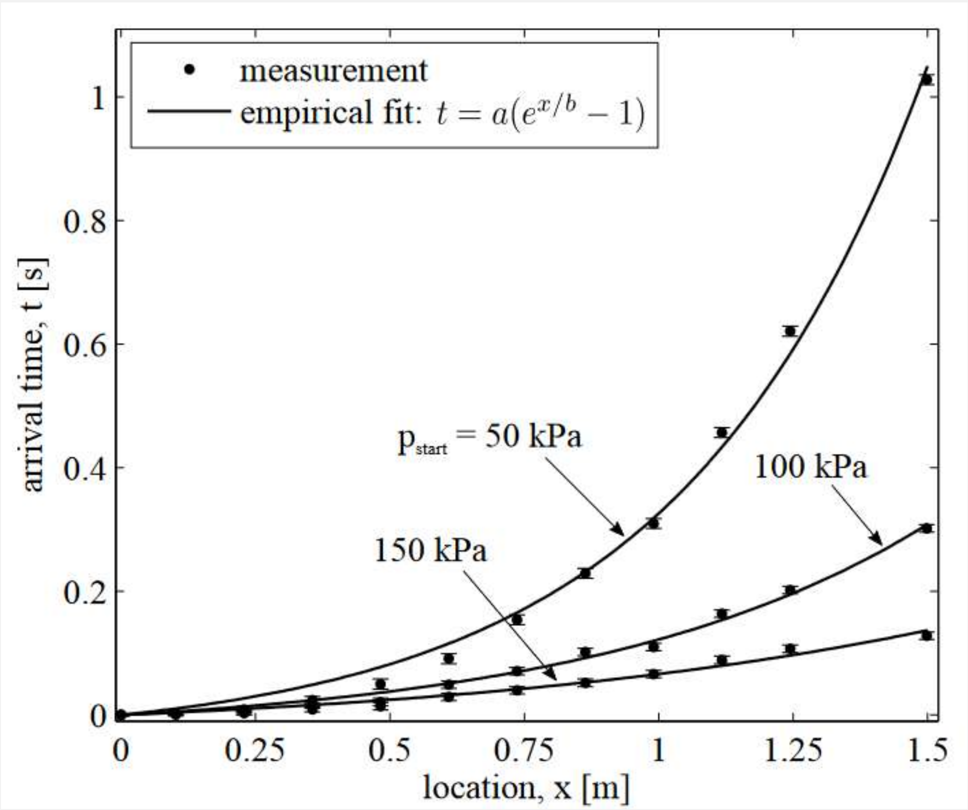

Conservation of mass model:

$$\left(\frac{\Delta x}{\Delta t}\right)\bigg|_x = \frac{\dot{m}_{in} - \pi D \int_0^x \dot{m}''_{dep}(X,t)\,dX}{\frac{\pi D^2}{4}\rho|_x}$$

Int J Heat Mass Transf 2016;96:573–81; ***Int. J. Heat Mass Transf*** 2016;98:728–37

Modified experimental setup using a helical tube system

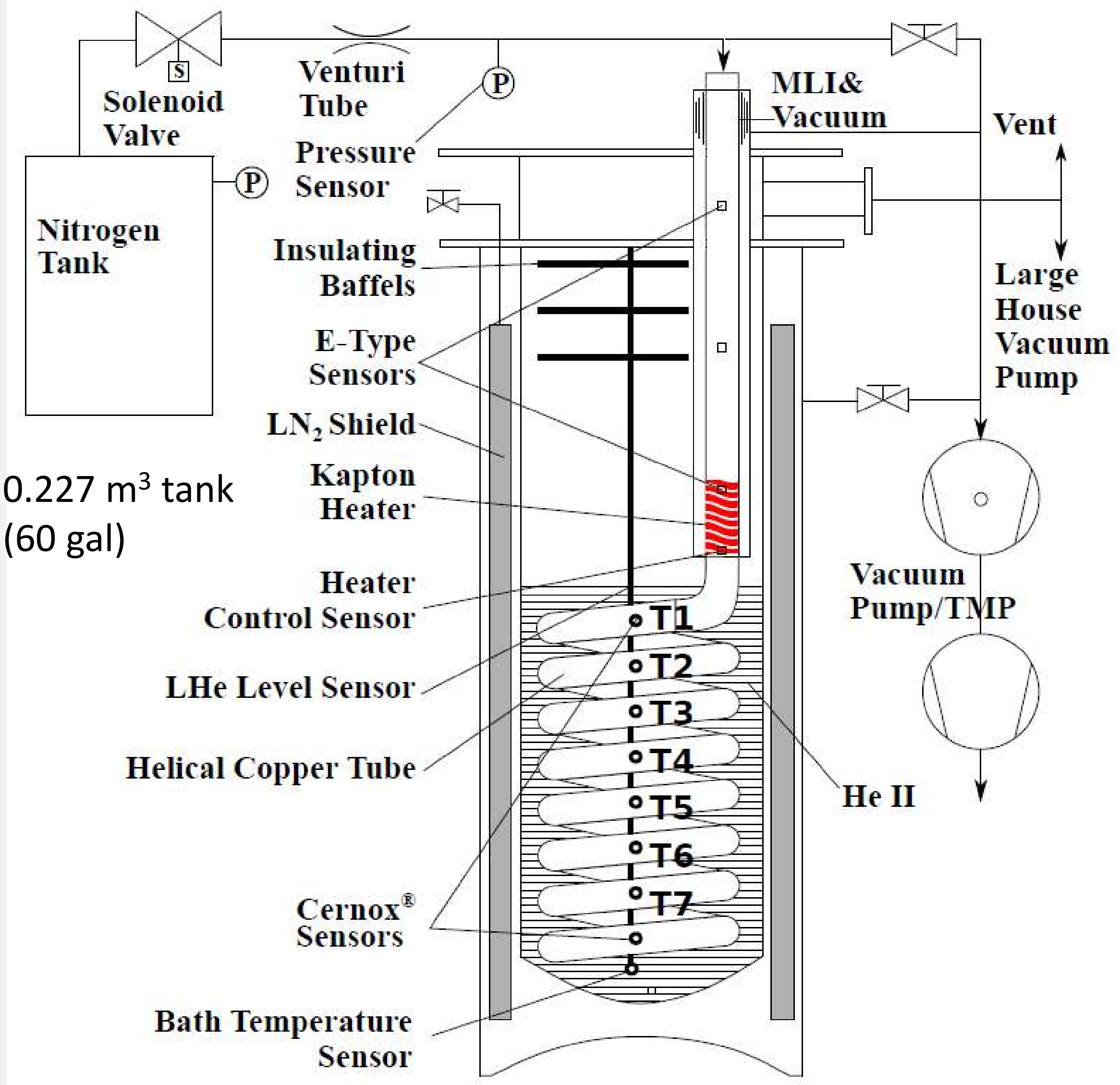

0.227 m^3 tank (60 gal)

Typical result for gas propagation in He I and He II cooled tube

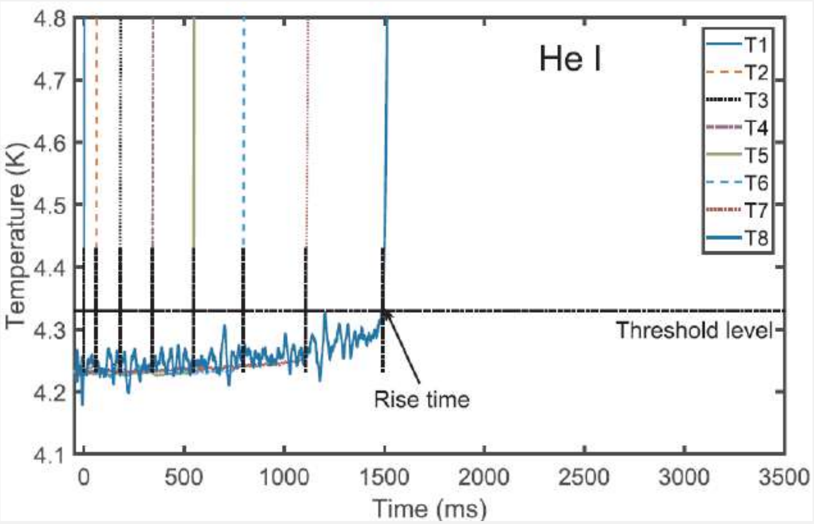

Temperature over time curves at different sensor sites

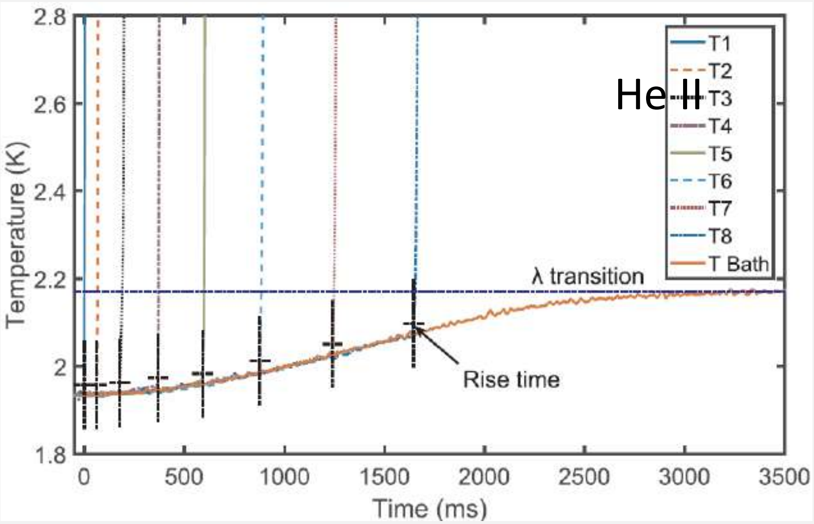

Risetime over position for He I and He II experiments

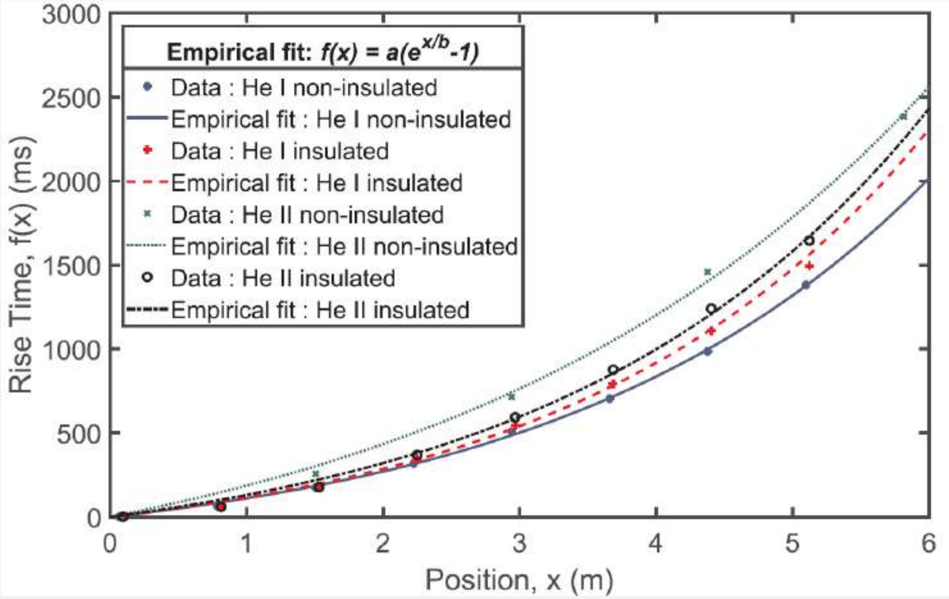

Cryogenics 2019; 100, 92–96.

Exponential slowing down of the condensable gas

- A 1-D finite deference model that systematically describes the fluid flow, heat transfer and mass deposition of a propagating and condensing gas inside a liquid helium cooled tube has been established.

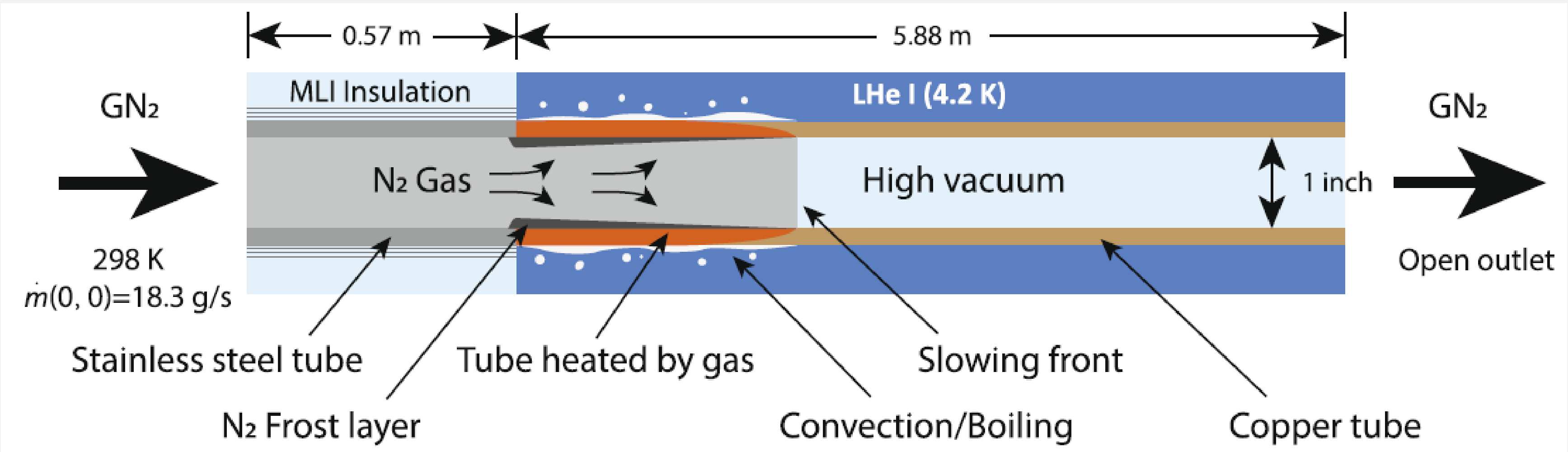

1. GN2 is treated as an ideal gas: $PM_g = \rho_g R T_g$ viscosity and gravity are neglected ;
2. An experimentally measured initial temperature profile is used for the insulated inlet section;
3. Steady-state heat transfer in LHe as the onset time of film boiling is very short;
4. The inlet mass flow rate is determined based on the measured pressure change in the tank;
5. The GN2 flow velocity assumed to be at the local speed of sound at the inlet.

Numerical model – Mass, momentum, and energy conservation

- The equations that describe the gas propagation in a long pipe cooled by helium:

Mass conservation: $$\frac{\partial \rho}{\partial t} + \frac{\partial}{\partial x}(\rho u) = -\frac{4}{D_1}\dot{m}_c$$

Momentum conservation: $$\frac{\partial}{\partial t}(\rho u) + \frac{\partial}{\partial x}(\rho u^2) = -\frac{\partial P}{\partial x} - \frac{4}{D_1}\dot{m}_c u$$

Energy conservation:

$$\frac{\partial}{\partial t}\left[\rho\left(\varepsilon + \frac{1}{2}u^2\right)\right] + \frac{\partial}{\partial x}\left[\rho u\left(\varepsilon + \frac{1}{2}u^2 + \frac{P}{\rho}\right)\right] = -\frac{4}{D_1}\dot{m}_c\left(\varepsilon + \frac{1}{2}u^2 + \frac{P}{\rho}\right) - \frac{4}{D_1^2}\mathrm{Nu}\cdot k\left(T_g - T_s\right)$$

Mass deposition rate: $$\dot{m}_c = \sqrt{\frac{M_g}{2\pi R}}\left(\Gamma\sigma_c\frac{P}{\sqrt{T_g}} - \sigma_e\frac{P_w}{\sqrt{T_w}}\right)$$

Radial heat transfer: $$\rho_w C_w \frac{D_2^2 - D_1^2}{4D_1}\frac{\partial T_s}{\partial t} = q - q_{He}\frac{D_2}{D_1}$$

$$q = \dot{m}_c\left[\frac{1}{2}u^2 + \hat{h}\left(T_g, P\right) - \hat{h}\left(T_s, P\right)\right] - \frac{\mathrm{Nu}\cdot k}{D_1}\left(T_g - T_s\right)$$

Numerical model – Radial heat transfer and heat transfer to LHe

- Simplified radial heat transfer model:

$$q_{\mathrm{dep}} = \dot{m}_c \left[\frac{1}{2} v^2 + h_{\mathrm{g}} - h_{\mathrm{s}} \right] + \frac{Nu \cdot k_{\mathrm{g}}}{D_1} (T_{\mathrm{g}} - T_{\mathrm{s}})$$

$$\rho_{\mathrm{SN}} C_{\mathrm{SN}} \delta \frac{\partial T_{\mathrm{c}}}{\partial t} = q_{\mathrm{dep}} - q_{\mathrm{i}}$$

$$\rho_{\mathrm{w}} C_{\mathrm{w}} \frac{D_2^2 - D_1^2}{4D_1} \frac{\partial T_{\mathrm{w}}}{\partial t} = q_{\mathrm{i}} - q_{\mathrm{He}} \frac{D_2}{D_1} + \frac{D_2^2 - D_1^2}{4D_1} k_{\mathrm{w}} \frac{\partial^2 T_{\mathrm{w}}}{\partial x^2}$$

Sieder-Tate correlation:

$$\mathrm{Nu} = 0.027 \mathrm{Re}^{4/5} \mathrm{Pr}^{1/3} \left(\frac{\mu_g}{\mu_s} \right)^{0.14}$$

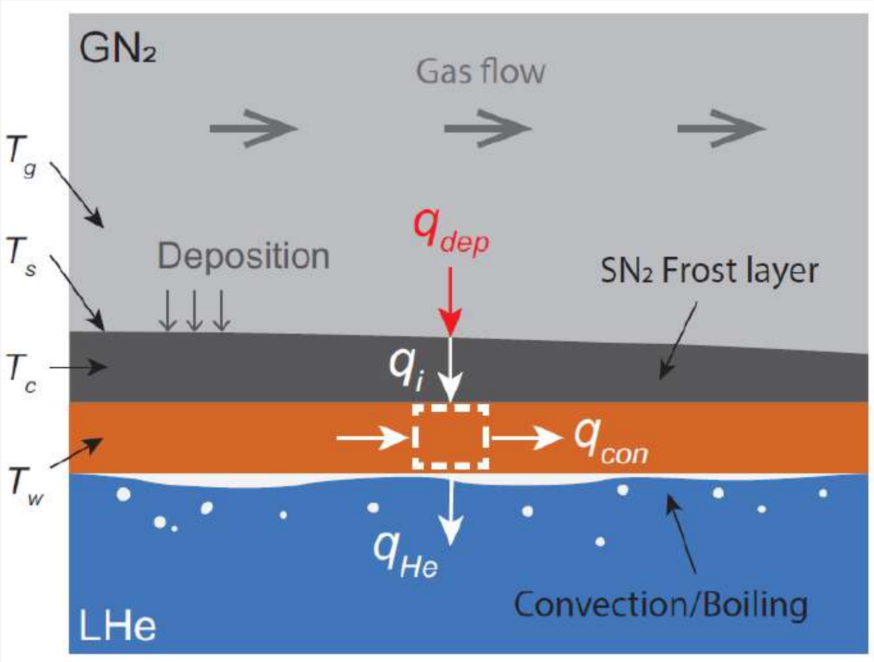

- Detailed information about the numerical model can be found in: ***Int. Heat Mass Transf.*** 129 (2019) 1144–1150; ***Int. Heat Mass Transf.*** 146 (2020), 118883; ***Int. Heat Mass Transf.*** 181 (2021) 121885.

Numerical model – Heat transfer in the LHe side

- Heat transfer correlations of He I:
- Heat transfer correlations of He II:

Tuning parameter

$$q_{\mathrm{He}} = B_{\mathrm{w}} \Delta T_{\mathrm{w}}^{5/4}$$

$$q_0^*(T_{bath}, x) = \left(\frac{2\psi}{D_2/2} \int_{T_{bath}}^{T'(x)} \frac{dT}{f(T)} \right)^{1/3}$$

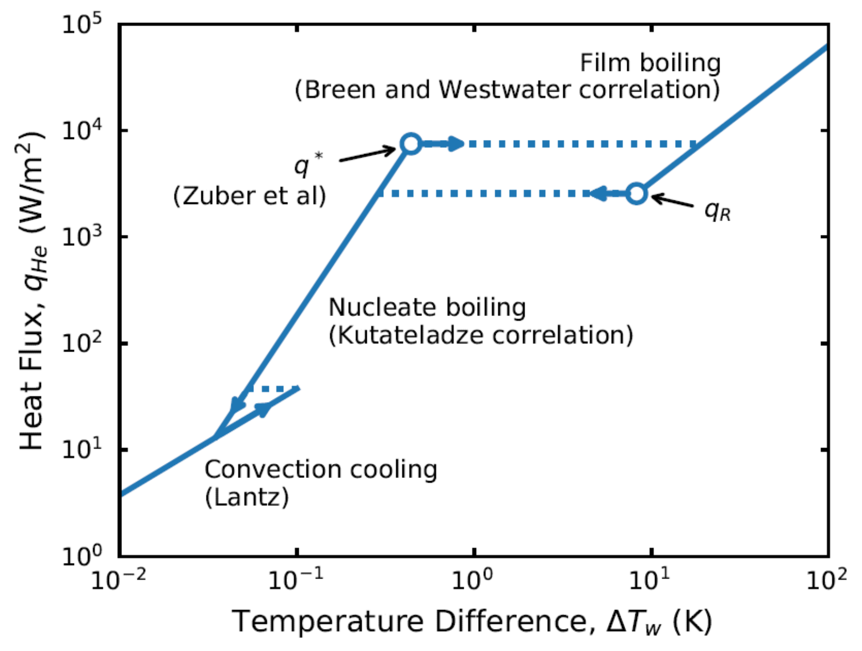

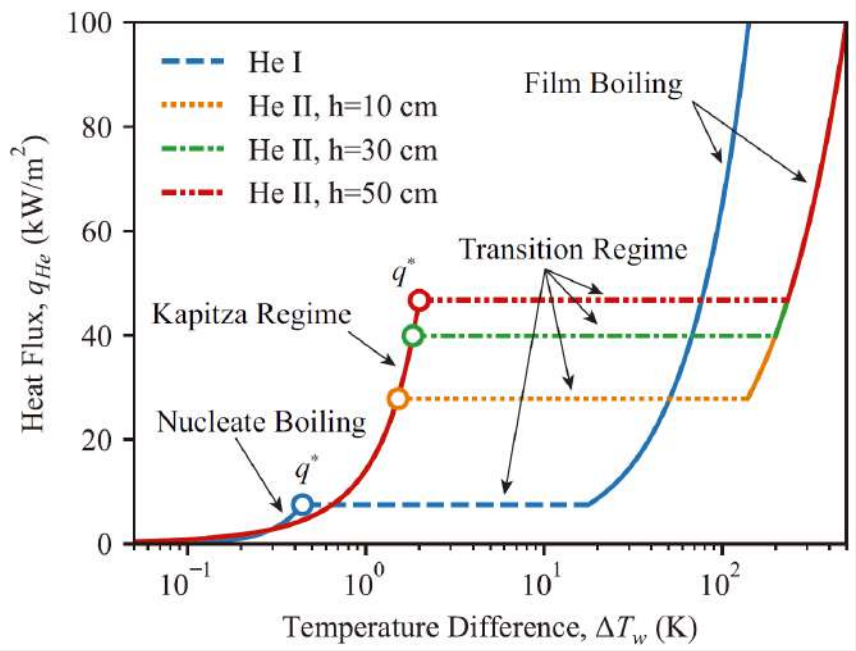

Model validation with the experimental results for He I

- We see a good agreement for the results with different mass flow rate with a single value of B_w parameter.

Threshold Level 4.7 K

B_w= 0.021 W/(cm^{2}K$^{5/4}$)

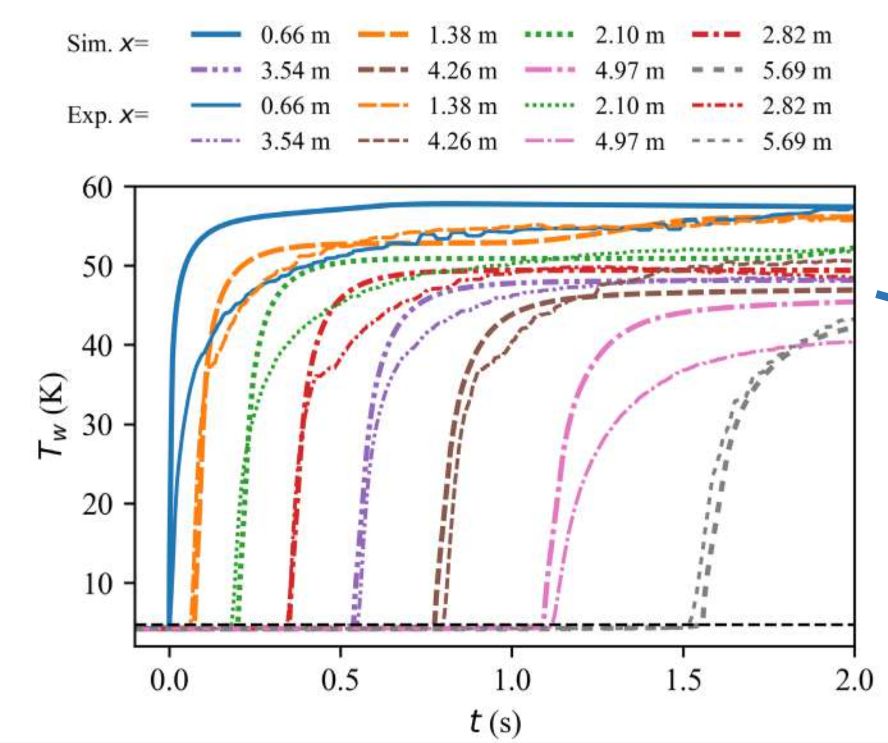

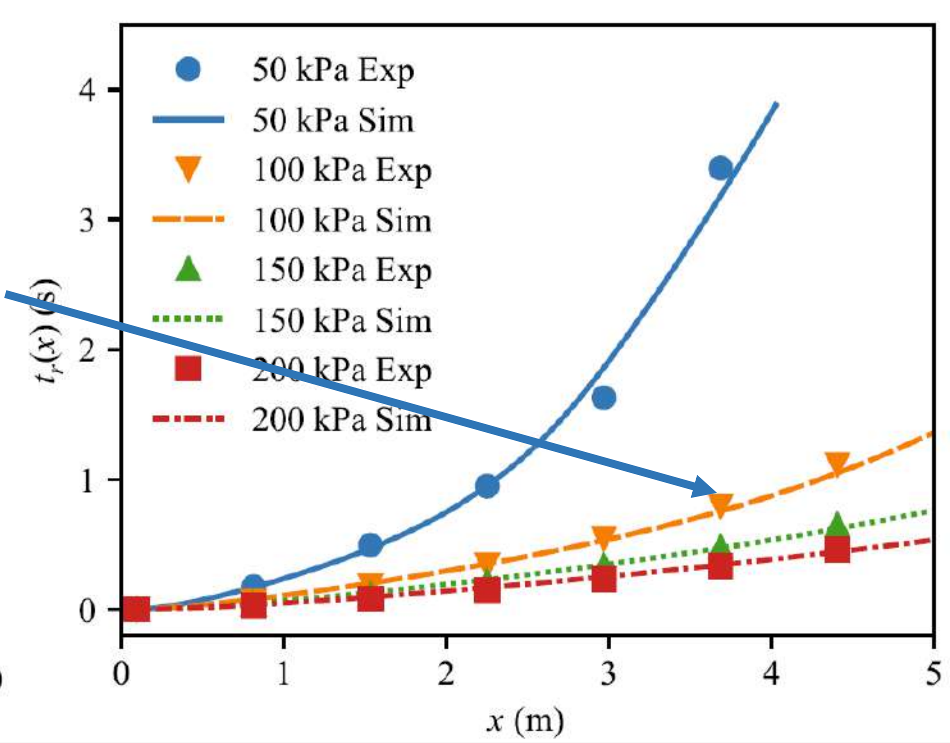

Model validation with the experimental results for He II

- The heat transfer condition varies greatly with different mass flow rate. We introduced an other tuning parameter ψ to the peak heat flux model which represents the derivation of the situation from an ideal cylindrical geometry.

Tank Pressure (kPa)	Optimal ψ
50	0.43
100	0.59
150	1.97
200	1.96

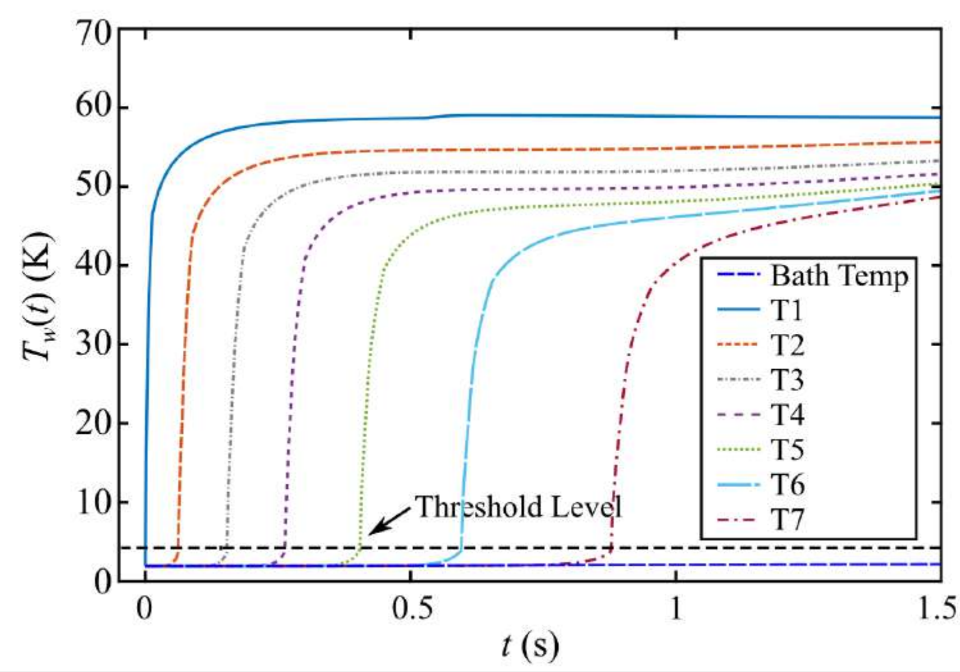

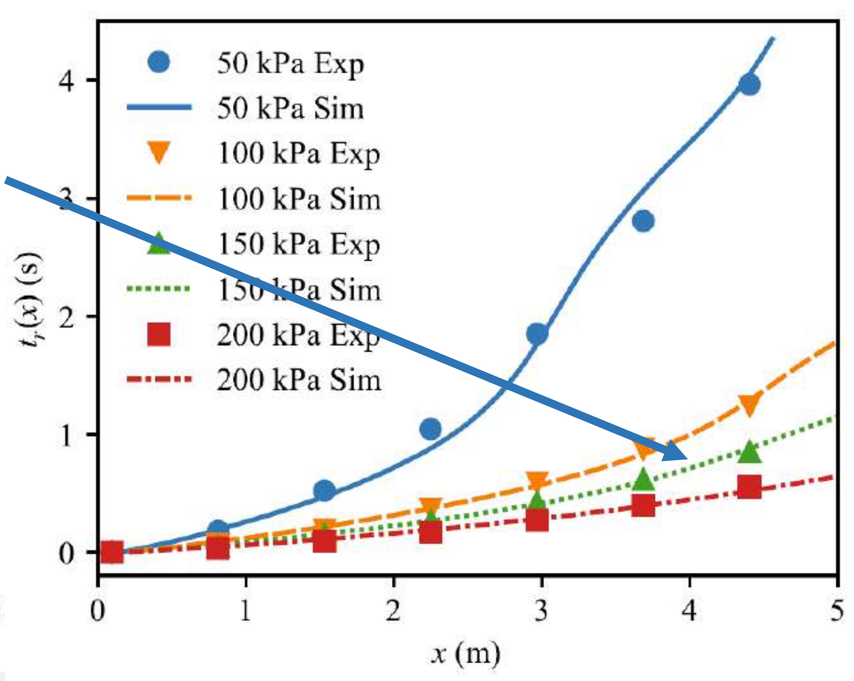

Definition of the freeze-out point for He I and He II case

- The freeze-out length is the upper limit of the propagation of possible contaminant, which can be evaluated with our 1D numerical model
- By analyzing the arrival time of gas front at each position, the freeze-out point can be defined by a linear fitting

Linear fitting: R^2>0.996

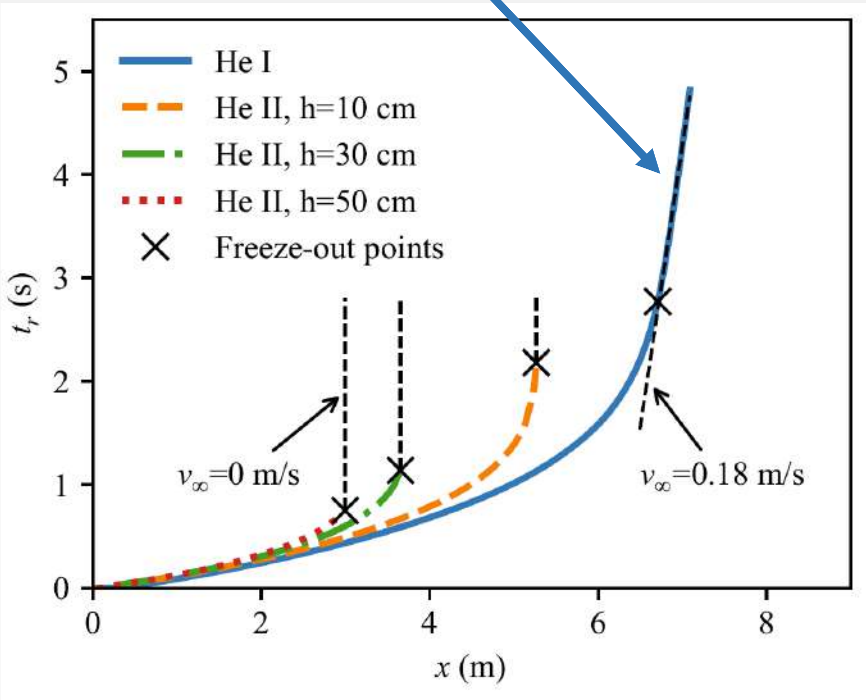

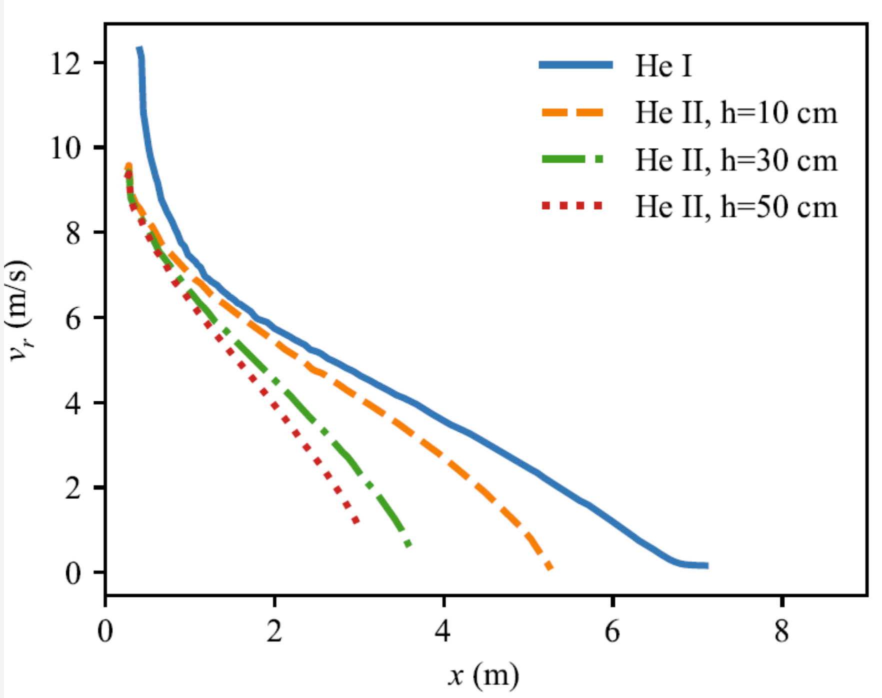

Empirical formula for the freeze-out length

For He I cooled tube

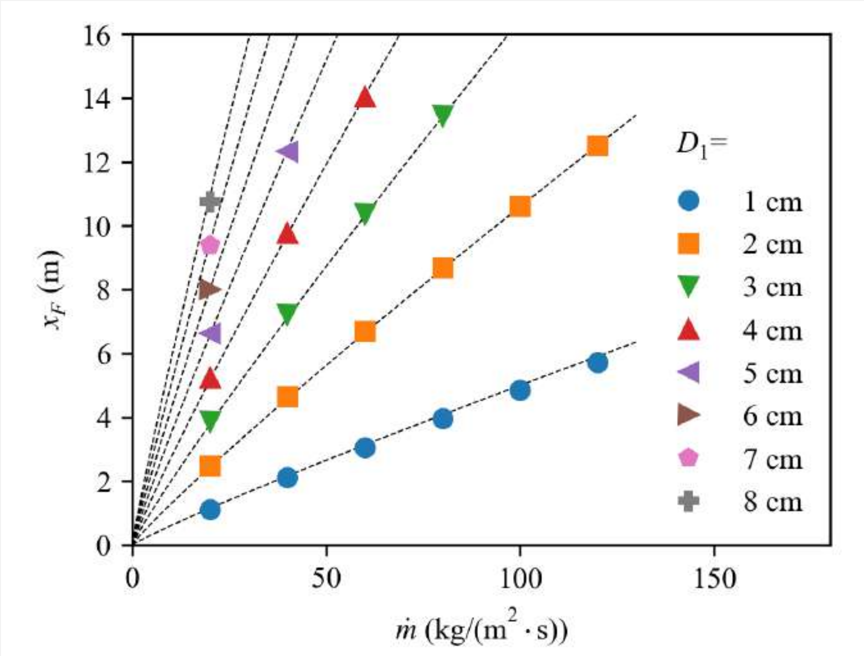

For He II cooled tube (T=1.9 K, h=50 cm, ψ=1)

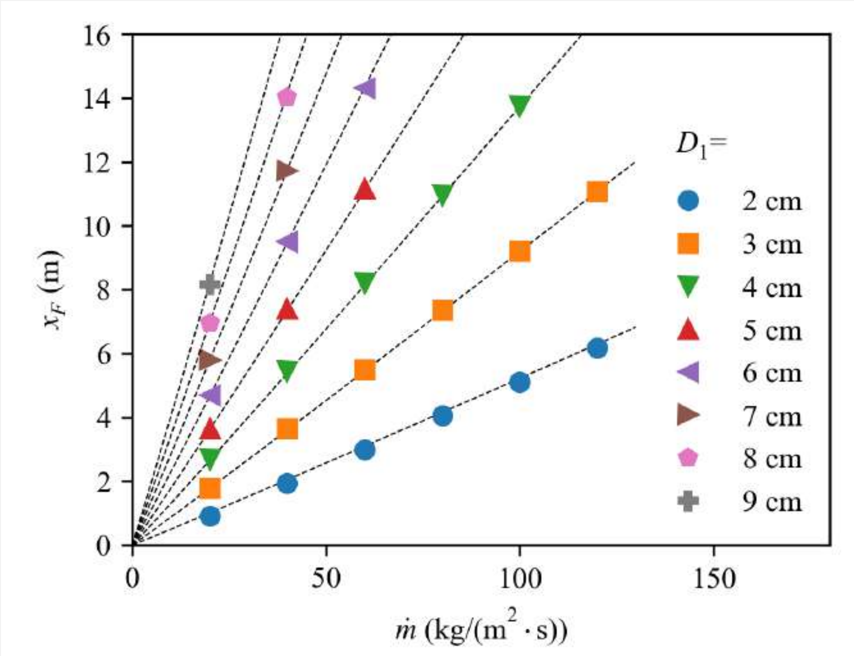

Empirical Formula:

$$x_F = aD_1^b\dot{m}^c$$

Parameter	Optimal value for He I	Optimal value for He II	Unit
a	0.074077	0.01786765	$m^{2c-b+1}kg^{-c}s^{c}$
b	0.91460513	1.02281107	1
c	1.08364073	1.39491514	1

⑤

Recent and Future development

⑤ Obtain and imaging ultra high turbulence with He II

- Liquid helium-4 has extremely small kinematic viscosity:

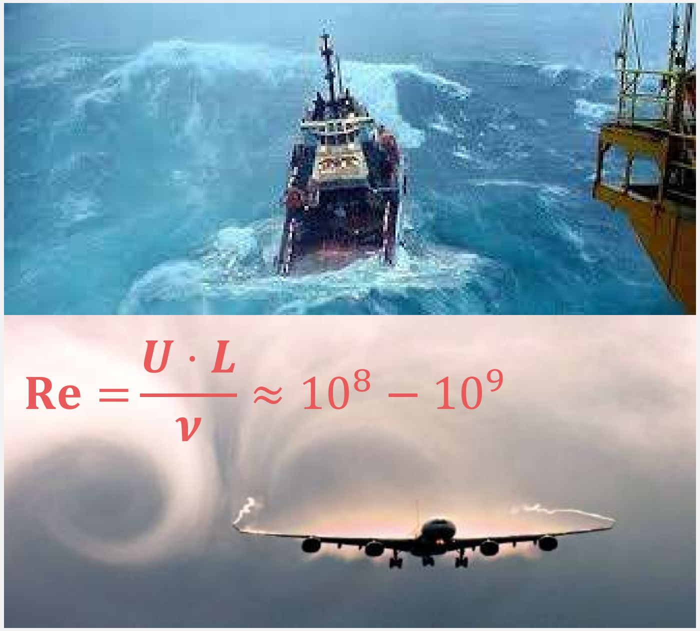

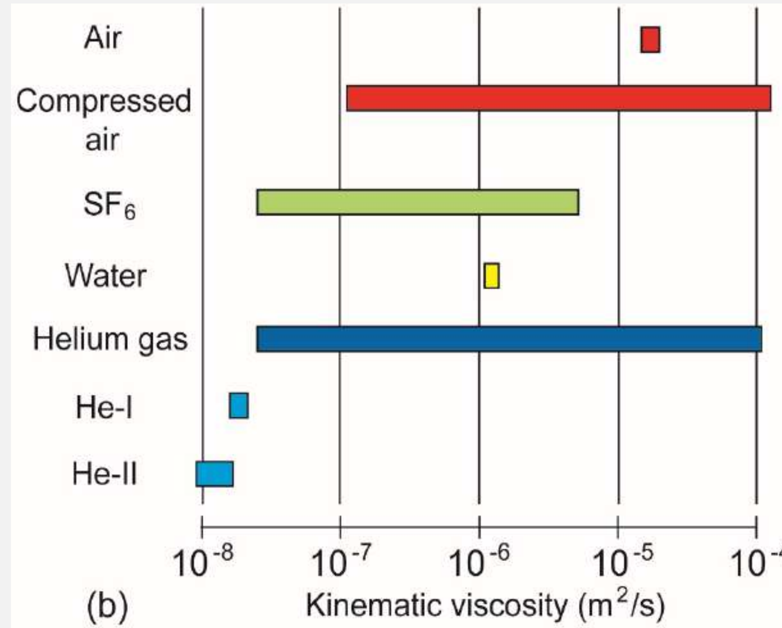

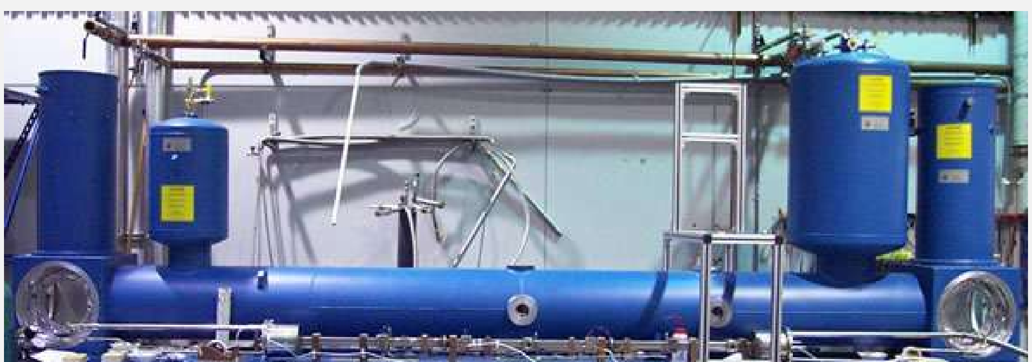

- Channel flows with Re~10^7 has already been achieved in our cryogenics lab in He-II.

1. High turbulence test facility in NHMFL

- Additional fs-laser beam path has been developed to created 2 tracer lines with adjustable distance, this upgrade will enable the 2D full field flow visualization.

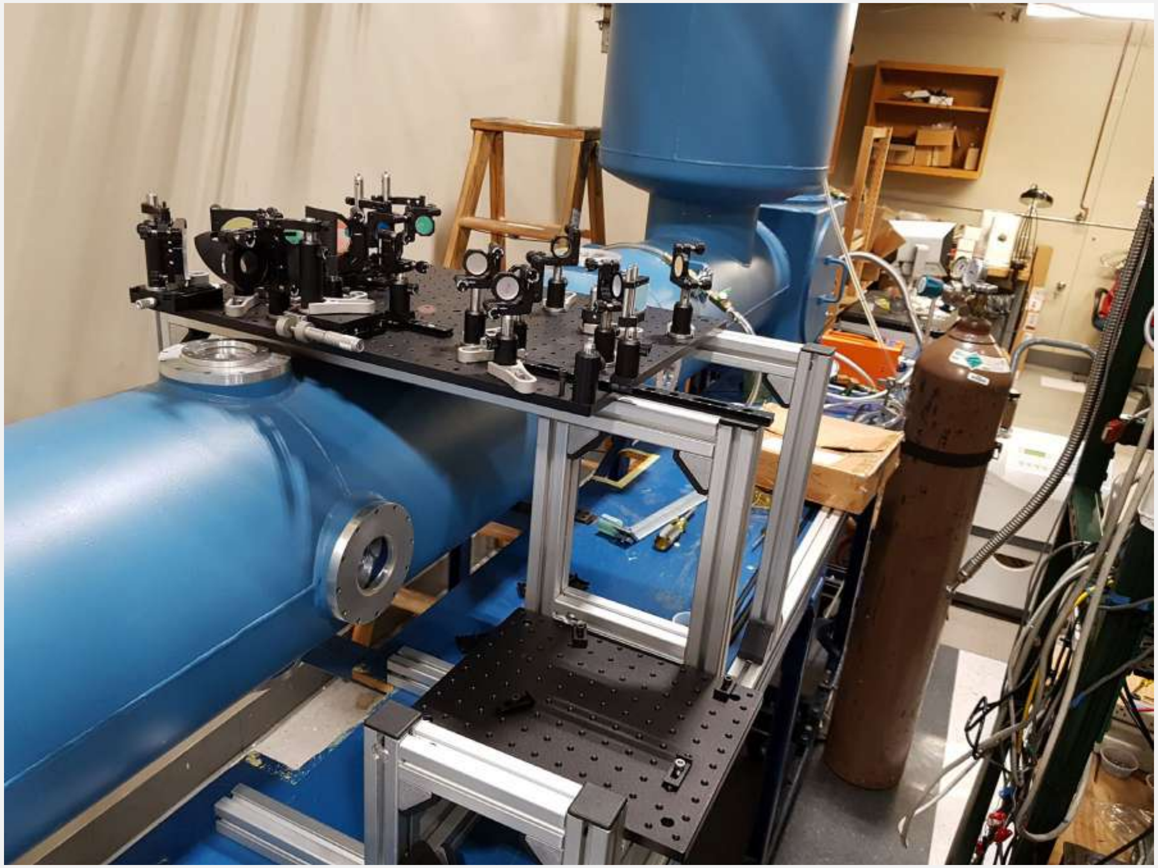

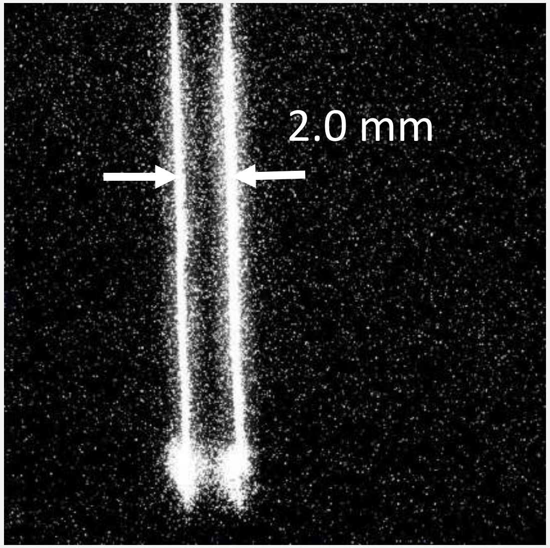

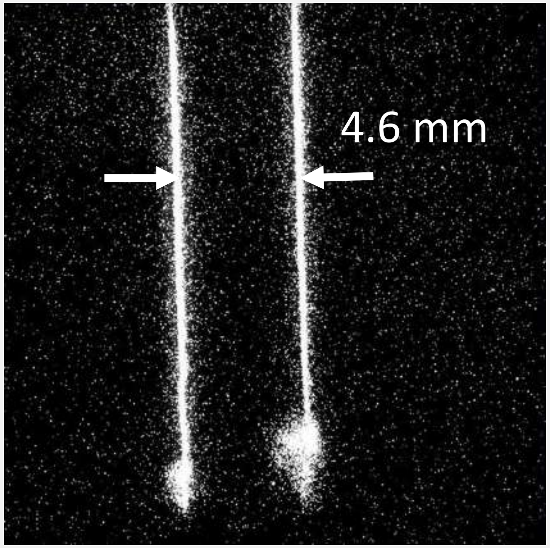

2. PIV/PTV with He_2^* clouds created by He3-neutron absorption

- Thermal neutron absorption on He3 atoms leads to the production of small clusters of helium molecules.

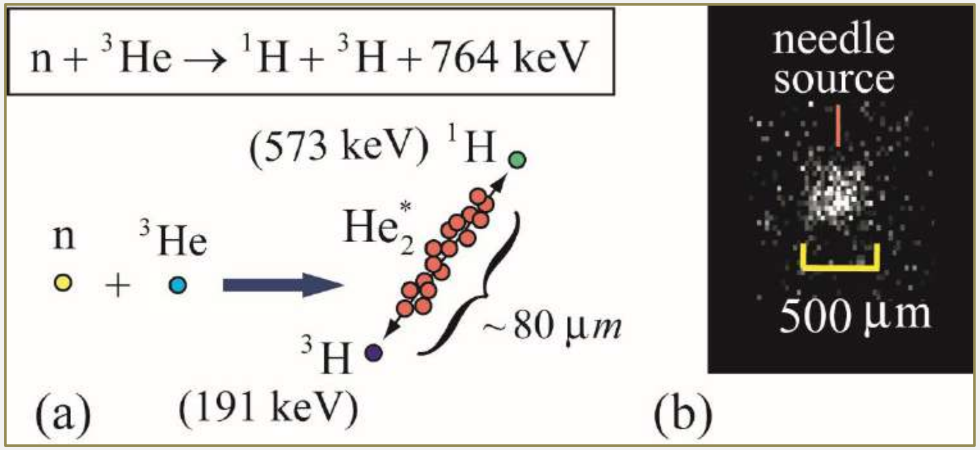

Cloud density can be tuned by changing He3 concentration or neutron flux.

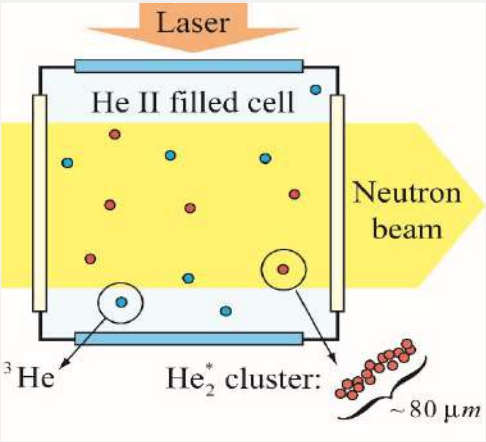

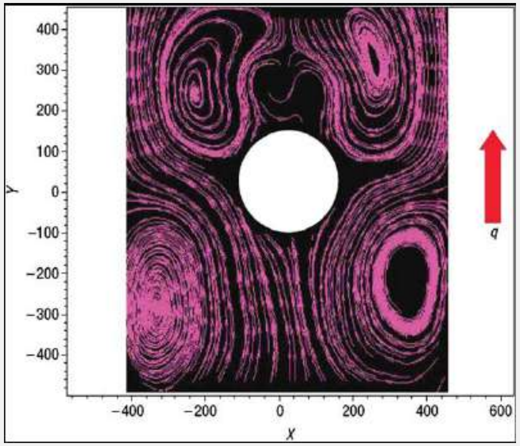

⑤ 2. PIV/PTV with He_2^* clouds created by He3-neutron absorption

- Collaboration with researchers at Oak Ridge and Univ. Tennessee:

Prof. M. R. Fitzsimmons, Prof. Xin Tong, et al

OAK RIDGE National Laboratory

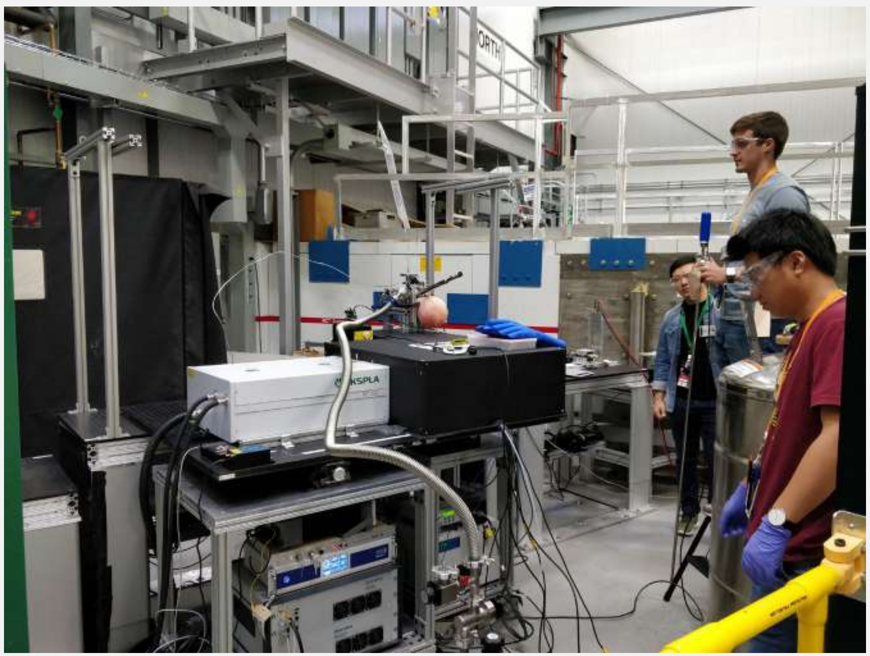

- He_2^* clouds created by He3-neutron absorption has been successfully visualized, 1st report has been published on PRL.

2. PIV/PTV with He_2^* clouds created by He3-neutron absorption

Distributions of (a) integrated intensity and (b) size of events recorded in a field of view

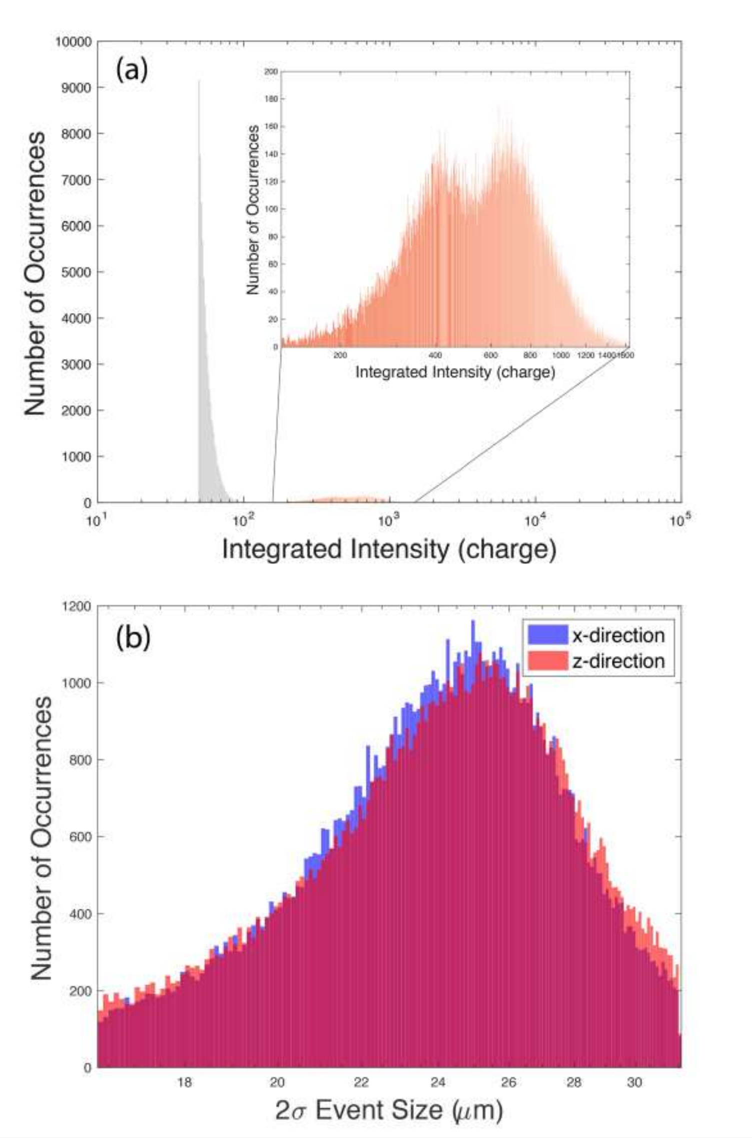

The net fluorescence signal integrated over the camera's field of view as a function of time

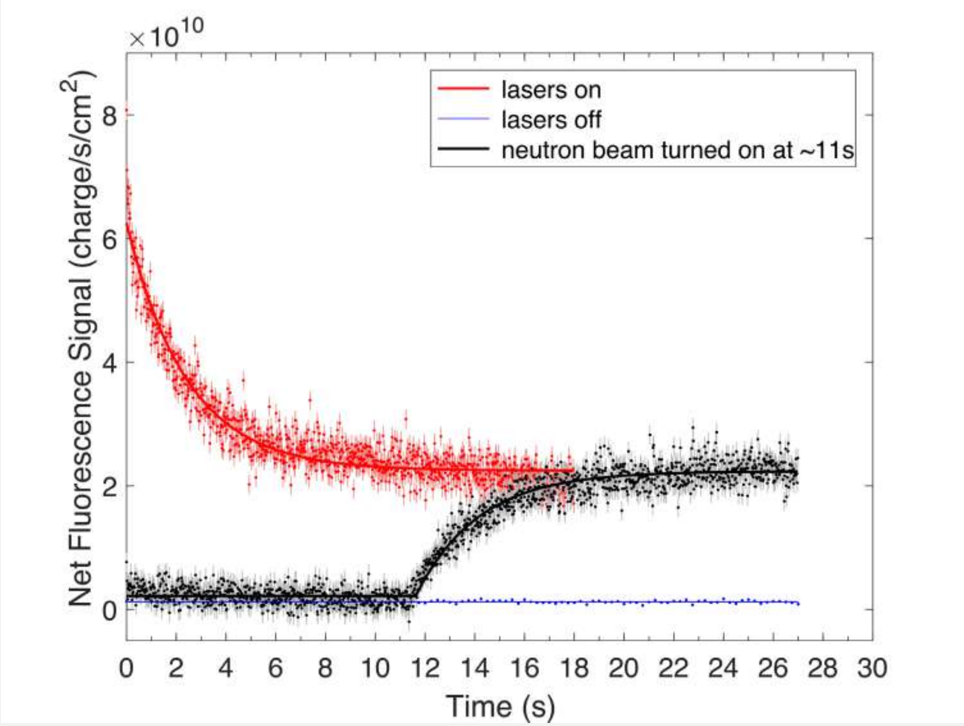

Reference

[1] N. Garceau, S.R. Bao, W. Guo, Heat and mass transfer during a sudden loss of vacuum in a liquid helium cooled tube - Part III: Heat deposition in He II, International Journal of Heat and Mass Transfer. 181 (2021) 121885. https://doi.org/10.1016/j.ijheatmasstransfer.2021.121885.

[2] S.R. Bao, W. Guo, Transient heat transfer of superfluid 4He in nonhomogeneous geometries: Second sound, rarefaction, and thermal layer, Phys. Rev. B. 103 (2021) 134510. https://doi.org/10.1103/PhysRevB.103.134510.

[3] Y. Tang, S.R. Bao, W. Guo, Superdiffusion of quantized vortices uncovering scaling laws in quantum turbulence, Proc Natl Acad Sci USA. 118 (2021) e2021957118. https://doi.org/10.1073/pnas.2021957118.

[4] S.R. Bao, T. Kanai, Y. Zhang, L.N. Cattafesta, W. Guo, Stereoscopic detection of hot spots in superfluid 4He (He II) for accelerator-cavity diagnosis, Int. J. Heat Mass Transf. 161 (2020) 120259. https://doi.org/10.1016/j.ijheatmasstransfer.2020.120259.

[5] H. Sanavandi, S. Bao, Y. Zhang, R. Keijzer, W. Guo, L.N. Cattafesta, A cryogenic-helium pipe flow facility with unique double-line molecular tagging velocimetry capability, Rev. Sci. Instrum. 91 (2020) 053901. https://doi.org/10.1063/5.0008117.

[6] X. Wen, S.R. Bao, L. McDonald, J. Pierce, G.L. Greene, L. Crow, X. Tong, A. Mezzacappa, R. Glasby, W. Guo, M.R. Fitzsimmons, Imaging fluorescence of He2* excimers created by neutron capture in liquid helium II, Phys. Rev. Lett. 124 (2020) 134502. https://doi.org/10.1103/PhysRevLett.124.134502.

[7] S.R. Bao, N. Garceau, W. Guo, Heat and mass transfer during a sudden loss of vacuum in a liquid helium cooled tube – Part II: Theoretical modeling, International Journal of Heat and Mass Transfer. 146 (2020) 118883. https://doi.org/10.1016/j.ijheatmasstransfer.2019.118883.

[8] B. Mastracci, S.R. Bao, W. Guo, W.F. Vinen, Particle tracking velocimetry applied to thermal counterflow in superfluid 4: Motion of the normal fluid at small heat fluxes, Phys. Rev. Fluids. 4 (2019) 083305. https://doi.org/10.1103/PhysRevFluids.4.083305.

[9] S.R. Bao, W. Guo, Quench-spot detection for superconducting accelerator cavities via flow visualization in superfluid helium-4, Phys. Rev. Applied. 11 (2019) 044003. https://doi.org/10.1103/PhysRevApplied.11.044003.

[10] N. Garceau, S.R. Bao, W. Guo, Heat and mass transfer during a sudden loss of vacuum in a liquid helium cooled tube – Part I: Interpretation of experimental observations, International Journal of Heat and Mass Transfer. 129 (2019) 1144–1150. https://doi.org/10.1016/j.ijheatmasstransfer.2018.10.053.

[11] N. Garceau, S. Bao, W. Guo, S. Van Sciver, The design and testing of a liquid helium cooled tube system for simulating sudden vacuum loss in particle accelerators, Cryogenics. (2019).

[12] S.R. Bao, W. Guo, V.S. L’vov, A. Pomyalov, Statistics of turbulence and intermittency enhancement in superfluid 4He counterflow, Phys. Rev. B. 98 (2018) 174509. https://doi.org/10.1103/PhysRevB.98.174509.

Thank you !

srbao@zju.edu.cn